[Frontiers in Bioscience 8, s1118-1139, September 1, 2003]

THE TRANSFER OF PROTONS IN WATER WIRES INSIDE PROTEINS

Samuel Cukierman

Department of Physiology, Loyola University Medical School, 2160 South First Avenue, Maywood, IL, 60153, USA.

TABLE OF CONTENTS

1. ABSTRACT

The translocation of protons across membrane proteins is an essential phenomenon in biology. Only in recent years however, have we started to study in detail some of the basic features of proton transfer in water molecules inside proteins at the single molecule level. Due to their truly unique features, gramicidin-based ion channels have been used to probe proton transfer in both experimental and computational fronts. In this article, some of the new experimental findings on proton transfer in water molecules inside proteins will be reviewed. The results, their interpretations, and the perspectives toward the understanding of structure-function illations of proton transfer in proteins are discussed.

2. INTRODUCTION

The main objective of this article is to review recent experimental findings and hypothesis concerning the modulation of proton transfer in water molecules inside proteins. Even though the transfer of protons in proteins is an essential phenomenon in biology, few experimental models are available in which all of the following conditions are met:

1. the structure of the protein is relatively simple and well known;
2. it is possible to measure directly proton transfer in a single molecule;
3. proton transfer can be manipulated experimentally, and
4. proton transfer can be studied using computational models in molecular dynamics.

Most of this review will focus on proton transfer in the gramicidin A ion channels. Even though it has been known for a long time that protons permeate gramicidin A channels at high rates (1-3), only in recent years has the usefulness of these channels been acknowledged as experimental and computational models for proton transfer.

This review starts by pointing out the general importance of protons in biology. The seminal role of protons in bioenergetics is discussed as well as the ideas and concepts regarding proton transfer in bulk water and water wires. A description of gramicidin A channels and methods used to measure single channel currents will also be discussed and followed by the analysis of experimental studies of proton transfer in these channels. Finally, a number of questions and future directions will be addressed. Because there is virtually no single biological process in which protons are inert, it is not possible to review in a comprehensive manner the role of protons in biological processes. Whenever possible, recent reviews (including those in this volume) on proton transfer in various systems will be mentioned. In particular, a very detailed review by DeCoursey has recently appeared (151).

3. PROTONS ARE ESSENTIAL FOR LIFE, BUT THEIR CONCENTRATION MUST BE TIGHTLY CONTROLLED IN VARIOUS BIOLOGICAL COMPARTMENTS

Among all ions, protons have the largest charge density. This property responds for the high reactivity of protons. In fact, free protons are found only in vacuum or dilute gases (4). In liquids, protons are solvated by water molecules. Protonation of specific chemical groups in biological macromolecules usually leads to conformational changes in the structures of those molecules. These may have a significant impact on various physiological or pathophysiological processes. Because of its high reactivity in biochemistry, the concentration of protons ($[H^+]$) in biological compartments like the cytoplasm, intracellular organelles or extracellular space must be controlled within narrow limits. Several homeostatic mechanisms are available for this control: from molecules in solution that act simply as chemical buffers to sophisticated membrane proteins that translocate protons between distinct cell compartments.

The movement or transfer of protons across biological membranes, and in distinct enzymes or protein complexes, has been studied or identified in various systems. For example:

1. Voltage-activated transmembrane H+ currents with presumably distinct physiological roles were measured in various cells (5,6). In particular, the need of H+ channels in the function of phagocytes has been recently shown (150);

2. The basic mechanisms by which protons are transferred in carbonic anhydrase (an essential enzyme that catalyzes the reaction H2CO3 ↔ CO2 + H2O) have also been studied in considerable detail (7);

3. Even though the flow of H+ across the bacterial membrane provides the energy source for the propulsion of bacteria, the details of this process remain unknown (8).

One of the most important categories of enzymes involved in the translocation of protons across membranes is the proton-ATPases (H^+-ATPases). These enzymes are generally grouped in two broad categories: the V- and F-ATPases.

Vacuolar or V-ATPases are present in several intracellular organelles and membranes. These enzymes use the energy released by the hydrolysis of ATP to pump H^+ from a compartment in which the H^+ electrochemical potential is low to a contiguous compartment in which the H^+ electrochemical potential is significantly larger. This transport occurs across a membrane. The function of V-ATPases is linked to many essential physiological processes that include accumulation of neurotransmitters in the presynaptic vesicles in nerve cells, egg fertilization, control of bacterial infections, etc. (9).

A second category of H^+-ATPases is comprised by the F-ATPases. F-ATPases share an overall similar structural organization with the V-ATPases (10-12). However, in contrast to V-ATPases F-ATPases *synthesize* ATP using the electrochemical gradient of protons that is present across a biological membrane. F-ATPases are present in chloroplasts and mitochondria. Interestingly, these organelles contain genes that encode some of the subunits of the F-ATPase. F-ATPases are also found in the cell membrane of bacteria where they trigger ATP synthesis. Evidently, life as we know would not have been possible without H^+-ATPases.

The synthesis of ATP is ultimately driven by the translocation of protons across a membrane. This translocation occurs inside highly specialized and extremely complex membrane proteins. The production of ATP in bacterial cells, mitochondria, and chloroplasts follows two distinct steps. First, H^+ are pumped out of the bacterial cell, the mitochondrial matrix, or the chloroplast stroma in animal or plant cells, respectively. This active extrusion of H^+ creates a transmembrane electrochemical gradient for H^+ across the cell membrane in bacteria and across the inner mitochondrial or thylakoid membranes in higher organisms (13). The second step consists in using that transmembrane H^+ electrochemical gradient to synthesize ATP. In this review, we will refer to proteins involved in either the pumping of H^+ across a membrane or in letting H^+ move against its electrochemical gradient (passive diffusion) as bioenergetic proteins.

3.1. Proton transfer in bioenergetic proteins occurs in a H-bonded network that is comprised of water and side chain residues of polar aminoacids

Our knowledge of the crystal structure of various bioenergetic proteins has increased tremendously in recent years. In particular, the various proton pathways inside those proteins appear to share some common organizational features:

1. High resolution structures of the reaction center from Rhodobacter sphaeroides suggest that a network of H-bonded water molecules and polar side chains of aminoacids underlie the transfer of protons from the cytoplasm to the quinone QB buried inside the protein (14,15). This pathway extends over a distance of

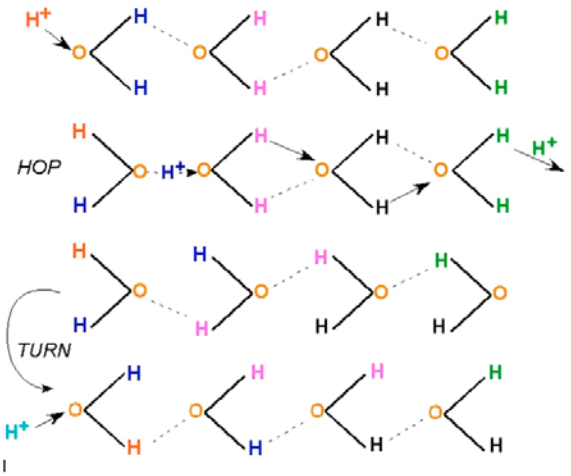

Figure 1. A schematic diagram of proton transfer in a water wire by a hop and turn mechanism Grotthuss's mechanism). See text for detailed explanation.

approximately 25 Å from the protein interior to the cytoplasmic side of the protein;

2. In cytochrome c oxidases, two distinct proton conduction pathways were identified (K and D channels). The K channel extends from the bulk aqueous phase on the electronegative side (bacterial cytoplasm) to the heme-copper center of the protein. This pathway transfers protons within a H-bonded network consisting of water molecules and highly conserved Lys, Thr, and Tyr residues (16-21);

3. An extensive H-bonded network between water molecules and the polar side chains of aminoacids (Arg, Asp, Tyr, Glu and Asp) has been identified in the extracellular region of bacteriorhodopsin. This network provides a pathway for the transfer of protons from the membrane surface to the buried retinal Schiff base (22);

4. Qualitatively similar H-bonded networks consisting of water and side-chain residues of polar aminoacids were also described in cytochrome f oxidases (23);

5. Even though a high resolution tridimensional structure of the proton pathway in the F0 subunit of the F0F1 ATP synthase is not yet available, it has been proposed that proton transfer through the F0 subunit is likely to involve a set of polar residues (Gln, Asn, Asp, His, Glu, Ser) located within its subunit a (24).

3.2. Proton translocation in hydrogenases

Hydrogenases are enzymes that synthesize or consume hydrogen gas (H_2). H_2 is essential to various forms of life that inhabit anaerobic environments (25). These enzymes, which seem to have been present in the earliest forms of life on Earth, were until recently thought to be present only in anaerobic bacteria whose energy metabolism is dependent on H_2. Today, it is known that hydrogenases are widely present among eukaryotes including our own genome (135,141). The production of H_2 in [Fe]-hydrogenases occurs in the reaction $2H^+ + 2e^- \leftrightarrow H_2$. A potential pathway for H^+ transfer from the enzyme surface to the catalytic center in this enzyme (~12 Å) was identified and is comprised of two Glu residues, one Ser residue, and a water molecule (26).

3.3. What is so peculiar to protons that makes them essential for the generation of ATP in living cells? Or, why did Nature 'choose' H^+ as the ion that triggers ATP production?

As mentioned above, a common phenomenon in virtually all cells is that a H^+ transmembrane electrochemical gradient is built up across a given membrane, and the movement of H^+ against this electrochemical gradient triggers the production of ATP. Is there anything so peculiar to the diffusion of protons in relation to other ions in water?

3.3.1. The mobility of protons in bulk water

The equivalent mobility or conductivity of protons in liquid *bulk* water is larger than of any other ion. The equivalent mobility of H^+ in acid solutions at infinite dilution and room temperature is ~$3.6 \cdot 10^{-3}$ cm^2 / (s·V·M). By contrast, the mobility of a K^+ which has an hydrated radius similar to $(H_3O)^+$ (3.3 versus 2.8 Å) is ~5-fold smaller. Considering that protons in solution are not free but associate with water molecules, and that $(H_3O)^+$ is the smallest possible protonated water cluster, it may be concluded that protons are not likely to diffuse hydrodynamically in water as with other ions (with the notable exception of OH^- which has a diffusion mechanism similar to H^+, see below). Even though the mechanistic details that determine the mobility of protons in bulk water are not yet completely understood, it is clear that in dilute acid solutions the H^+ mobility cannot be determined by the hydrodynamic diffusion of protonated water clusters. The term proton transfer in solutions is used to contrast with the classical hydrodynamic diffusion of other ions.

A special mechanism for the high mobility of protons in water has been proposed (27-29). This mechanism became known as Grotthuss's. The scheme in figure 1 illustrates the two basic features of a Grotthuss mechanism: the hop and turn steps. Consider 4 water molecules interconnected via H-bonds, and that there is an electrochemical proton gradient favoring the net movement of H^+ from left to right in figure 1. The approach of a proton (1^{st} line in figure 1) to an oxygen of a water molecule leads to the formation of a new covalent bond between these two atoms. Consequently, one of the protons that was covalently linked to the oxygen of that water molecule will now be shared with an adjacent water forming a protonated water dimer ($(H_5O_2)^+$, 2^{nd} line in figure 1). This hopping step propagates between adjacent water molecules in the water chain (2^{nd} line in figure 1). As the proton hops, the dipole moment of the water molecule donating the proton reverses by ~180^o. Once the proton leaves the last water molecule in the water chain of figure 1 (2^{nd} line), the total dipole moment of the chain is reversed (3^{rd} line in figure 1). If another proton must be transferred in the same direction as before, the four water molecules need to rotate back (turn step) to their original configurations (4^{th} line, figure 1; for a more detailed explanation and references see 30). Historically, the

rotation of water molecules has been considered the limiting step for proton transfer in bulk water (28,29).

The idea that the turn step in a classical Grotthuss mechanism is what limits the mobility of protons in bulk water has been cogently questioned by Agmon (32-34). Based on several experimental measurements, Agmon has argued that the limiting step of proton transfer in *bulk water* is *not* likely to be the rotation of water molecules. It was proposed that the disruption of a H-bond between waters located in the first and second solvation shells of $(H_3O)^+$ (32,34-36) is the rate limiting step in H^+ transfer. Molecular dynamics simulations of protonated water clusters have shown a continuous fluctuation between $(H_5O_2)^+$ and $(H_9O_4)^+$. These two protonated water clusters occur with approximately the same probability (36), and this would explain the high proton mobility in *bulk water*.

3.3.2. Water or Proton Wires

The concept of a proton or water wire is of particular interest to the study of proton transfer in proteins (31,37). This idea started with an initial suggestion by Onsager (see 31) who had considered the possibility that the side chains of polar aminoacids (like Ser, Thr, Tyr, Glu) could form a H-bonded network (Hydrogen Bonded Chain, HBC) that provides a hydrophilic environment for the transfer of ions across a membrane. The term proton wire was coined by Nagle and Morowitz (37) "*…in the expectation that HBCs could perform the same function for protonic circuits at the membrane micro scale that metallic wires perform for conventional electronic macro circuits…*" (31). In the past 7 years, the subject of how protons can be transferred in proton wires in general, and inside proteins or membranes in particular, attracted a considerable number of meaningful computational and theoretical studies (38-49). The H-bonded networks of water and polar side chain residues of aminoacids described above in the context of various bioenergetic proteins are proton or water wires. In contrast to bulk water molecules that are tetrahedrically coordinated, water molecules in a water wire are arranged in basically a 'single' dimension with a coordination number of 2-3. For example, each water molecule can donate two H-bonds (to an adjacent water molecule, and to the oxygen of a carbonyl group of the protein, for example) and receive an H-bond from another adjacent water molecule.

It has been proposed that the limiting step for proton transfer in water wires is the reorientation of water molecules (31). This is in accordance with computational studies of water wires inside gramicidin A channels (43).

3.3.3. Proton transfer in water wires occurs via two coupled mechanisms of charge movement

An important feature of proton transfer in water wires is that the transfer of one positive charge (H^+) by the hop-and-turn mechanism is accounted for by two distinct coupled mechanisms of charge movement. The transfer of a proton (hopping step) per se accounts for a fraction of the total charge transferred along the water wire (~ 67%, see 31 and references therein). This ratio depends ultimately on the specific chemical groups involved in this transfer. The remaining charge transfer is a consequence of the reorientation of the electron clouds of the water molecules (reorientation of the dipole moment). One way to reason about this phenomenon is to consider that the proton does not 'move' continuously along the H^+ electrochemical field (proton hops), and that the reorientation of dipole moments in water molecules involves the redistribution of the electronic clouds in water molecules (thus, a 'capacitive' charge movement).

4. A 'SIMPLE' EXPERIMENTAL AND THEORETICAL MODEL TO STUDY H^+ TRANSFER IN WATER WIRES INSIDE PROTEINS: GRAMICIDIN A (GA) BASED PROTON CHANNELS

Despite the impressive knowledge accumulated on the structure of bioenergetic proteins, the detailed mechanisms or dynamics by which proton transfer in these molecules occur are not known. Several factors or limitations may contribute to this lack of information. Among them are the facts that bioenergetic proteins are extremely complex structures and that there is a tight coupling between H^+ transfer and redox potentials (50). Moreover, H^+ transfer cannot be measured directly at the single molecule level in bioenergetic proteins. Thus, the motivation and need exist for developing a relatively simple model to study H^+ transfer in water wires in proteins at both the experimental and theoretical or computational levels. Our experimental model, on which we will concentrate throughout the rest of this review is based on the structure and on simple and discrete atomic modifications of gramicidin A (gA) channels.

gA is a highly hydrophobic pentadecapeptide secreted by *Bacillus brevis*. In lipid bilayers, its primary structure consists mostly of an alternating sequence of D- and L-aminoacids (HCO-*L*-Val-Gly-*L*-Ala-*D*-Leu-*L*-Ala-*D*-Val-*L*-Val-*D*-Val-(*L*-Trp-*D*-Leu)$_3$-*L*-Trp-NH-$(CH_2)_2$-OH). This primary structure defines a right-handed $\beta^{6.3}$ helix in which the side chain residues are in contact with the core of the lipid membrane, and the carbonyl and amide groups line the pore of the protein (51-55). The association via six intermolecular H-bonds between the amino termini of two gA peptides, each located in a distinct monolayer of a lipid membrane, results in the formation of an ion channel that is selective for monovalent cations (2, 55-57). Disruption of intermolecular H-bonds results in the dissociation of gA monomers with the consequent loss of ion channel function. In figure 2 the structure of native gA molecules as determined by solid-state NMR in micelles is shown (51; the pdb file of this structure can be downloaded from www.rcsb.org/pdb/, identification name, 1GRM). In this figure, gA channels are shown in the dimeric (functional channel in lipid membranes) form. gA channels are approximately 25 Å long with a cross sectional diameter of approximately 4 Å.

Of particular interest for the study of proton transfer is the fact that the pore of gA channels contains a single file of water molecules. The short diameter of the pore of gA does not allow the simultaneous presence at any given cross section of the channel of 2 water molecules or a

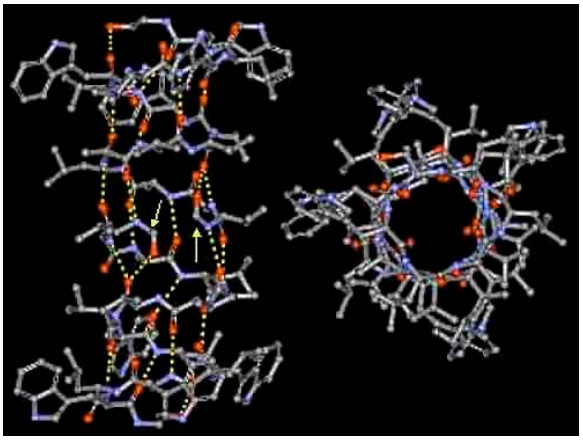

Figure 2. The structure of native gA channel in longitudinal and cross sections. The arrows point to the N-termini, which in gramicidin channels are formylated. H-bonds are represented by dashed yellow lines. The hydrogens were omitted for the sake of clarity. Carbons, oxygens, and nitrogens are represented by gray, red, and blue spheres, respectively.

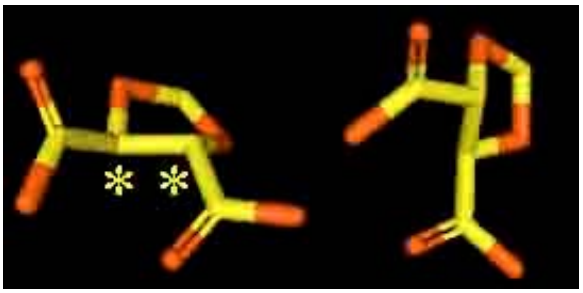

Figure 3. Energy minimized structures of the SS and RR diacid dioxolanes. Hydrogens were omitted for the sake of clarity. The orientations of the dioxolanes in this figure represent their approximate configuration in the SS or RR channels (see figure 4). Carbons and oxygens are represented by yellow and red spheres, respectively.

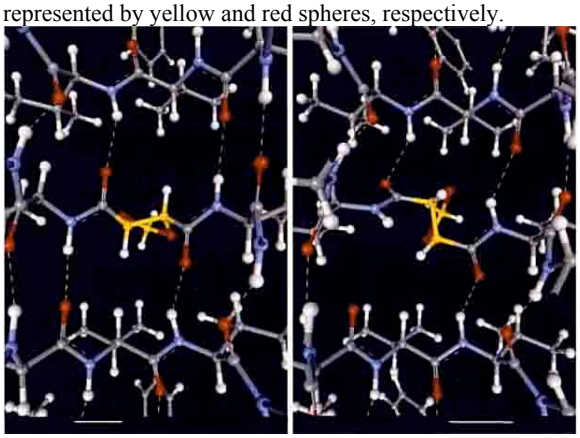

Figure 4. Energy minimized structures of the SS (left) and RR (right) –dioxolane linked gA channels (from reference 78 with permission). H-bonds are represented by dashed green lines. Carbons, oxygens, nitrogens, and hydrogens are represented by gray, red, blue, and white spheres, respectively. However, for the dioxolane linker only, carbons are represented by yellow spheres. See text for discussion.

water molecule and a monovalent cation. In gA channels, permeation of monovalent cations occurs via a no-pass or single file diffusion mechanism (58-63). While the presence of waters in the pore of gA channels is not questionable, it is not clear how many water molecules reside in the pore of the channel. Measurements of streaming potentials (63) in various alkaline chloride solutions at various concentrations suggested that approximately 7 water molecules are present in the pore of gA channels (60). On the other hand, it was also proposed (61) that 7-9 waters are present in the water wire in gA channels. Tripathi and Hladky (64) in an elegant communication have recently revisited this issue using a distinct and original experimental approach. Their experimental results also suggested that the gA pore contains on average 7 water molecules confirming some of the previous conclusions. It is of interest to note that in various studies of molecular dynamics in gA channels, 7-10 water molecules were equilibrated inside the pore of gA channels (43, 65-70).

4.1. Covalently linked gA channels

It is possible to dimerize gA molecules by covalently linking them via their amino termini to a molecular group. In fact, this was a seminal strategy originally developed by Urry et al. (72) to support the hypothesis that the functional gA channel in lipid bilayers is indeed a dimer of gA molecules. A recent and interesting discussion on the functional structure of gA channels in membranes was recently published (73,74). In the original study by Urry et al. (72; see also 75) malonic acid was the linker to which the amino termini of two desformylated gA molecules were attached. As predicted, malonyl-linked gA channels had a considerably longer open time than native gA channels. Other covalently linked gA dimers were also synthesized using as linkers glutaric acid (76), and the diacid dioxolane (77, see below).

In our work, we have been using the diacid dioxolane molecule to covalently link two gA peptides. This procedure was originally developed by Stankovic et al. (77). Because two chiral carbons (see figure 3) are present in the diacid dioxolane, two optical isomers of the dioxolane-linked gA channel can be synthesized: the SS and RR-dioxolane linked channels. For the sake of brevity, in this article these will be referred to as the SS and RR channels.

Figure 4 shows energy minimized structures of the SS and RR channels using molecular mechanics calculations (78). This figure shows a close-up, as viewed from inside the channel, at the junction between the amino termini of two gA molecules and the dioxolane. In the SS channel there is a constrained and continuous transition between the two gA $\beta^{6.3}$ helices (77,78). However, in the RR diastereoisomer of the dioxolane-linked gA channel a pronounced tilt of the dioxolane group by approximately 90^{o} (in relation to the SS channel) causes significant alterations in some of the H-bonds between the carboxy and amino groups that provides the secondary structure of the gramicidin A channel (77-79).

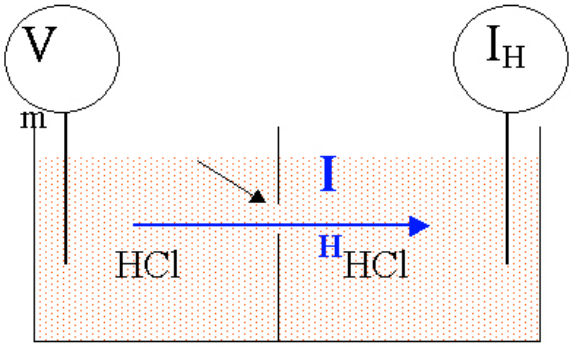

Figure 5. Diagram of the experimental set-up that is used to measure I_H in a single channel molecule. Notice that the hole in the partition in the middle of the chamber (arrow) is completely out of scale.

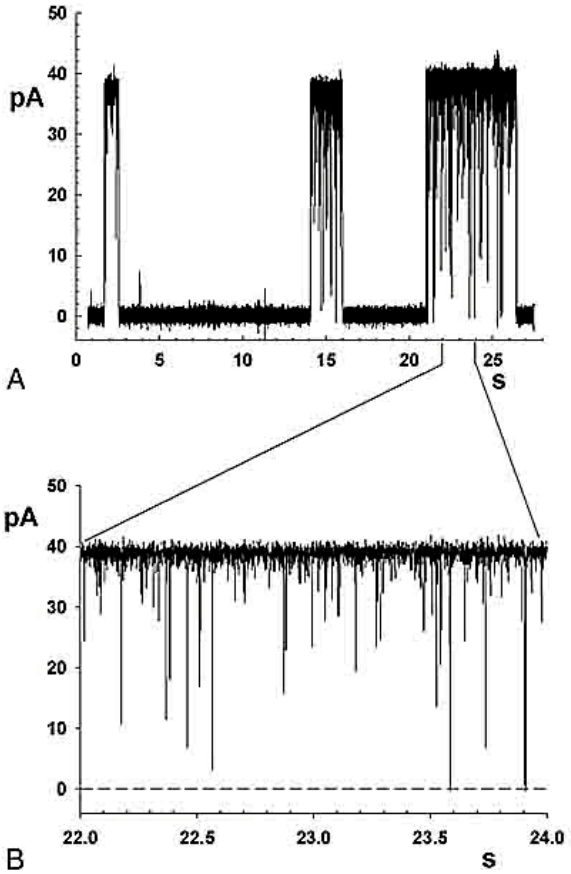

Figure 6. Recordings of proton currents through single native gA channels. Notice in panel A the formation and disappearance of 3 gA channels (they could be the same or different channels). Panel B expands the time scale of recordings in panel A between the 22nd and 24th seconds. See text.

Molecular dynamics simulations of the water wire inside (which is not shown in figure 4) native gA channels have shown that a given water molecule donates two distinct H-bonds to an adjacent water molecule and to an oxygen of a carbonyl group that lines the channel, and accepts one H-bond from the other adjacent water (see 3.3.2 above; 43). Because the H-bond network that holds up the structure of gA channels is significantly different between the SS and RR channels (39,40,78,79), it was reasoned that the transfer of H^+ in the water wires inside those channels might also have distinct kinetic properties.

5. MEASURING H^+ CURRENTS IN A SINGLE MOLECULE

Figure 5 shows a diagram of the experimental set-up that is used to measure directly H^+ currents through a molecule incorporated in a lipid membrane or bilayer. The chamber consists of two aqueous compartments separated by a plastic partition with a small (0.10 - 0.15 mm in diameter) hole. The channel forming protein is added to one of the compartments at a very low concentration ($\leq 10^{-12}$ M). This low concentration of channels in solution allows the incorporation of just a single channel in the bilayer.

Two basic experimental stimulation protocols are used in our studies. In one of them, a constant DC-voltage (V_m) is applied and electronically controlled (voltage-clamp) across the membrane. The resulting single channel proton currents (I_H) are monitored as shown in figure 6. This figure shows I_H from single native gA channels. Notice that there are two distinct modes of gating in native gA channels. In the first gating mode, the channel opens and closes with a relatively slow time course (several s). This 'slow' gating mode (see figure 6A) is caused by the association (H-bond formation between gA monomers, opening of channel) and dissociation (disruption of intermonomeric H-bonds, closing of the channel) of gA-gA monomers (see figure 2 above). The second gating mode, which is very fast, occurs inside the long duration of the open state of the native gA channel (see figure 6B which is a temporal expansion of figure 6A from t = 22 s to t = 24 s). This fast gating mode consists of fast closures (closing flickers) with an average duration of less than 100 μs (80,81). Notice that most of these closing flickers have very short durations and cannot reach the 0 pA baseline (where the channel is in the closed state). This lack of resolution is due to a relatively slow frequency response of the recording system (~ 5 kHz). This issue will be rediscussed in section 11.1. If the current amplitude of the open state of the channel is measured, by Ohm's law the single channel proton conductance can easily be calculated ($g_H = I_H / V_m$, g_H in single channels is usually expressed in picoSiemens, pS).

A second stimulation protocol consists of applying a voltage ramp across the bilayer. The top panel of figure 7 illustrates a voltage ramp from 0 to 340 mV in ~ 6 s. The middle panel of figure 7 shows I_H that flows through the channel in response to that voltage ramp. The bottom panel in figure 7 shows the I_H-V_m relationship. This stimulation protocol is particular advantageous for single channels that have prolonged open times as with covalently linked gA dimers. From plots like the one in the bottom of figure 7, the behavior of g_H can be immediately documented as a function of V_m. Notice that only the initial

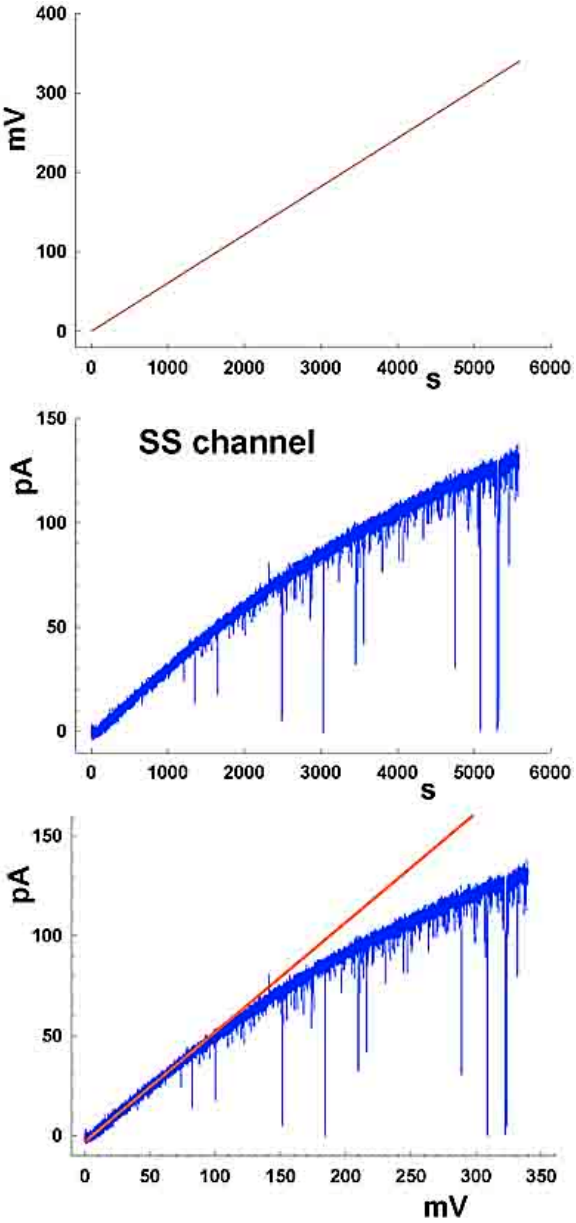

Figure 7. The upper and middle panels show the time courses of the voltage ramp and the single SS I_H, respectively. The I_H – V_m relationship for the single SS channel is shown in the bottom panel.

portion of the I_H - V_m relationship behaves in an ohmic (linear) manner. At larger V_ms, there is a tendency for I_H to saturate (see section 7.1).

6. PROTON TRANSFER AND NOT HYDRODYNAMIC DIFFUSION OF PROTONS OCCURS IN WATER WIRES IN VARIOUS GA CHANNELS

Before proceeding with the analysis of structure-function relationships of proton transfer in various gA channels, it is desirable to review the experimental measurements that buttress a special transfer mechanism for H^+ inside gA channels. These are:

1. gH in gA channels is 1-2 orders of magnitude larger than the single channel conductance for the second most permeable ionic species (Cs+) (1,2,81,82);

2. As discussed in section 4.1, gA channels are filled with ~7-10 water molecules. Ion permeation in gA channels occurs in a single file mode. The pore of a gA channel is ~4 Å, and a cation and water molecule cannot simultaneously occupy the same cross section of the channel. Consequently, the diffusion of ions inside the channel is accompanied by water flow. Levitt et al. (62) and Rosenberg and Finkelstein (63) demonstrated that the permeation of protons through native gA channels is not accompanied by water movement as with other permeant monovalent cations;

3. Tredgold and Jones (83) have determined the ratios between single channel conductances in native gA channels to various monovalent cations in either H2O or D2O solutions. Interestingly, these single channel conductances were 1.06 – 1.13 -fold larger in H2O than in D2O. These values are comparable to the ratio between the viscosities of H2O and D2O. By contrast, the kinetic isotope effects for H+ transfer in native gA (84,85), and in both the SS and RR-dioxolane linked gA dimers (85) were larger by 1.27 – 1.37 -fold. These kinetic isotope effects are similar to those measured in bulk solution (85). Moreover, because they are considerably larger than the ratios between single channel conductances to other monovalent cations in either H2O and D2O, a special transfer mechanism for H+ in various gA channels is supported. Figure 8 shows typical IH - Vm relationships for the SS and RR channel in either 1 M HCl or DCl. Notice that the ratios between the slopes of the linear portion of these relationships are 1.27 and 1.31 for the SS and RR channels, respectively;

4. The Gibbs's free energy of activation for proton transfer in various gA channels are in general smaller than those for single channel conductances to alkalines, and consistent with proton transfer (86, see section 9.1 below).

It seems reasonable to assume that H^+ is being transferred inside gA channels by a mechanism distinct from hydrodynamic diffusion.

7. PROTON TRANSFER IS MODULATED BY THE CHIRALITIES OF CARBONS IN THE DIOXOLANE LINKER

As discussed in 4.2 above, differences in conformation between the SS and RR dioxolanes in dioxolane-linked gA channels cause structural differences in the organization of H-bonds that maintain the secondary structure of gA channels (40,78,79). It was postulated that these could implicate in differences between the proton transfer properties in the SS and RR channels.

Some of the differences between the SS and RR channels are illustrated in figure 9 (78). Voltage ramps

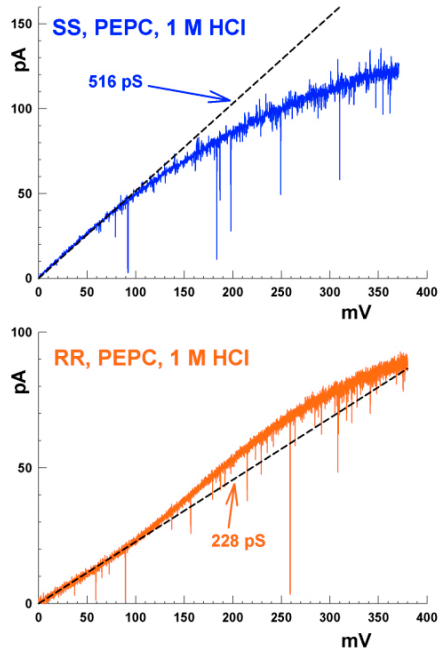

Figure 8. I_H – V_m or I_D – V_m plots for the SS and RR channels (from reference 85 with permission). The ratios between the linear parts of these plots are 1.27 (SS) and 1.31 (RR).

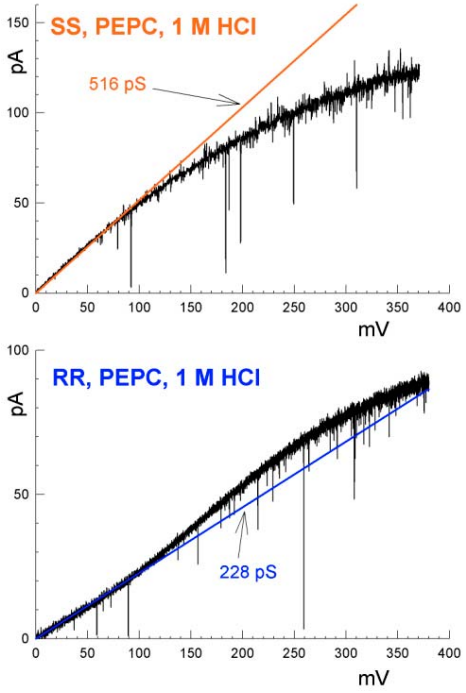

Figure 9. Distinct I_H – V_m plots for the SS and RR channels (from reference 78 with permission). See text for discussion.

from 0 to ~ 380 mV were applied across the SS or RR channels reconstituted in a lipid bilayer made of a mixture of 80% PE (1-palmitoyl 2-oleoyl phosphatidylethanolamine) and 20% PC (1-palmitoyl 2-oleoyl phosphatidylcholine) using decane as the solvent. The results illustrated in figure 9 were obtained in 1 M HCl.

At relatively low V_ms (0 - ~100 mV in figure 9; see also figure 8), the I_H - V_m plots are linear for both the SS and RR channels. In this linear region, g_H in the RR channel (228 pS) is significantly smaller than in the SS channel (516 pS). The I_H - V_m relationship for the SS channel is sublinear (at relatively large voltages I_H is smaller than the value predicted by the initial ohmic relationship, see graph) and tends to saturate at large V_ms. By contrast, I_H - V_m plots for the RR channel are hyperlinear and also tend to saturate at large transmembrane voltages. It is remarkable that a simple alteration in the stereochemistry of the dioxolane causes meaningful alterations in proton transfer in the water wire in dioxolane-linked gA channels.

8.THE DEPENDENCE OF H^+ TRANSFER ON PROTON CONCENTRATION ($[H^+]$) IN BULK WATER AND IN THE VARIOUS GA CHANNELS IN MONOGLYCERIDE BILAYERS

One approach to understand the properties of H^+ transfer in various gA channels is to study its dependence to $[H^+]$. These studies were initially performed in bilayers composed of glycerylmonoolein (Δ 9 *cis* monoolein) in decane (GMO/decane bilayers). The structure of GMO is shown in figure 10. In acidic solutions, phospholipid bilayers (common biological membranes) are positively charged. GMO bilayers are electrically neutral over a wide range of $[H^+]$, and this in principle facilitates the initial analysis of experimental results. Even though studies of H^+ transfer in various gA channels were also performed in phospholipid membranes (85-87), this review will focus on studies performed in monoglyceride bilayers.

Figure 11 (top graph) shows log (g_H) – log ($[H^+]$) relationships for the SS (blue circles), the RR (pink squares), and native gA channels (green triangles). It should be pointed out that unless otherwise mentioned that the g_H values used in these graphs were obtained from the initial linear (ohmic) segment of I_H - V_m relationships (see figures 7-9). A brief look onto figure 11 (top graph) leads to the conclusion that the $[H^+]$-dependencies of g_H in native gA channels, and in the SS and RR channels, are dramatically different.

8.1. Proton transfer in water

Before attempting to interpret the complex plots in the top panel of figure 11, it is instructive to analyze the dependence of proton conductivity (Λ_H) in bulk water on $[H^+]$. This is shown in the bottom graph in figure 11. In this graph, Λ_H values were plotted against $[H^+]$ (brown triangles) or thermodynamic activity (red triangles) in log-log scales. There is a linear dependence between log (Λ_H) and log ($[H^+]$) within the $[H^+]$ range of 1 - 2000 mM. The slopes of these relationships are 1.00 or 0.96 depending on whether proton activities or $[H^+]$ are used, respectively. These slopes indicate that: a) Λ_H is limited by diffusion of protons in water, and b) that a proton diffuses or is transferred as a single charge 'moving' independently of

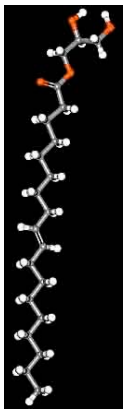

Figure 10. Energy minimized structure of a GMO molecule. Hydrogens, carbons, and oxygens are represented by white, gray, and red spheres, respectively.

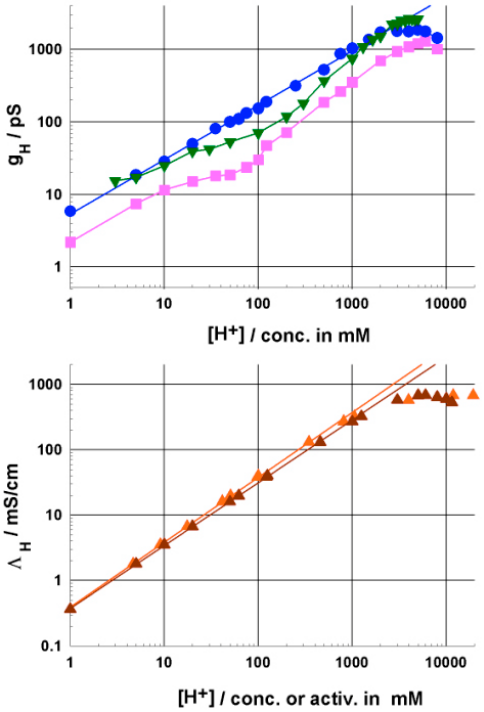

Figure 11. Log-log plots of g_H versus $[H^+]$ (from reference 30 with permission). See text for discussion.

other charges, *ie.*, proton current in bulk solution is a function of $[H^+]^1$. This plot in itself does not allow the conclusion that protons are transferred (like in figure 1 for example), or diffuse hydrodynamically. Other experimental approaches must be used to distinguish between these possibilities (see below and section 6.1). Notice also that at $[H^+] > \sim 2$ M, Λ_H saturates and declines.

In figure 12, the equivalent mobilities of protons (μ_H) were plotted as a function of $[H^+]$. Notice that: a) μ_H is the *equivalent* proton mobility, *ie.*, proton mobility is normalized by the $[H^+]$ in bulk solution. Having this point in mind, it is important to clarify the apparent contradiction between the bottom graph in figure 11 and figure 12. Λ_H increases with $[H^+]$ because the concentration of protons (charge carriers) is increasing in solution, and so the solution conductivity. However, the average equivalent mobility (μ_H) decreases due to increased electrostatic interactions between the conducting ions in solution, *ie.*, in very dilute solutions these interactions are minimized. In figure 12, the value of the self-diffusion coefficient of H_2O (88) is represented by the horizontal dashed line. The self-diffusion coefficient of H_2O is used as an approximation to the self-diffusion coefficient of $(H_3O)^+$ which is the *smallest possible* protonated water cluster. Notice that μ_H is considerably larger than the self-diffusion coefficient of H_2O over a wide range of $[H^+]$. This strongly suggests that a special transfer mechanism underlies the high μ_H in aqueous solutions.

However, at $[H^+] > 2$ M, there is a marked decrease in μ_H. At very high [HCl], μ_H approaches and becomes smaller than the value of the self-diffusion coefficient of H_2O. This suggests that in concentrated acids, the probability of proton transfer decreases, and μ_H is given essentially by the hydrodynamic flow of protonated water clusters (85,89-93).

Considering the subtleties inherent to a proton transfer mechanism like the one depicted in figure 1, the attenuation of Λ_H at high $[H^+]$ is hardly surprising. In order for H^+ transfer to occur by a Grotthuss mechanism, a particular geometrical arrangement between water molecules is required (86, see 9.1 below). The structures of hydrated H^+ and Cl^- change as [HCl] varies. As [HCl] increases, new H-bonds between Cl^- and H^+ will be formed, H-bonds between $(H_3O)^+$ and adjacent water molecules will decrease, the number of water molecules solvating $(H_3O)^+$ will also decrease, and the probability of finding a Cl^- between water molecules in a water wire increases. Those factors will contribute to obliterate H^+ transfer in the water wire. Taken together, these effects will decrease the probability of proton transfer by a Grotthuss-type mechanism and, the equivalent mobility of protons will be strongly attenuated in high [HCl] solutions (89,90): H^+ transfer is then likely to occur by hydrodynamic diffusion of protonated water clusters.

8.2. Proton transfer in various gA channels

The log (g_H) – log ($[H^+]$) relationship for the SS channel in figure 11 (top graph) is qualitatively similar to the log (Λ_H) - log ($[H^+]$) plot in aqueous solutions. However, the slope of that relationship for the SS channel is considerably smaller than 1.00. Within 1 – 2000 mM range of $[H^+]$ there is a linear dependence between log (g_H) and log ($[H^+]$). The slope of this line is 0.75 ($g_H \alpha [H^+]^{0.75}$). The conclusion is that in the $[H^+]$ range of 1 - 2000 mM, the rate limiting step for g_H is *not* diffusion in bulk solution but in the channel itself or at the channel-membrane/solution interfaces. An interesting and still intriguing observation is that at very low concentrations of $[H^+]$, it is expected that g_H be determined by diffusion limitation of protons in solution, and as such the initial slope of the curve that relates log (g_H) to log ($[H^+]$) should be 1.00. This does not occur under several experimental conditions (94).

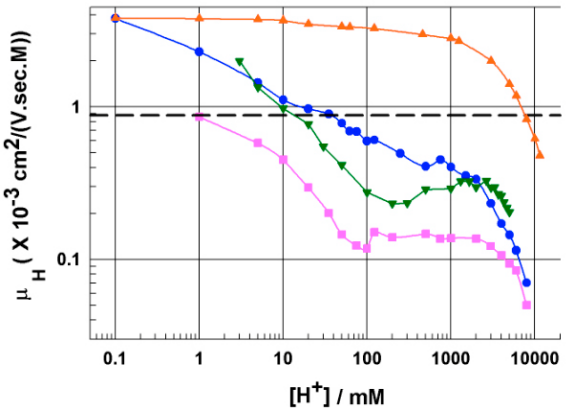

Figure 12. The equivalent proton mobilities in water (red triangles), SS (blue circles), native gA (green triangles), and RR (pink squares) channels (from reference 30 with permission). The dashed lines indicate the self-diffusion coefficient for H_2O. See text for discussion.

At 2 M < $[H^+]$ < 5 M, g_H saturates around 1750-1850 pS, and for $[H^+]$ > 5 M, g_H declines. The similarity at high [HCl] between this plot and the bottom graph in figure 11 suggests that g_H is limited by proton diffusion in solutions (both bulk and at the channel-membrane/solution interface, see below).

An implicit assumption in the interpretation of results like those shown in figure 11 that is not often recognized concerns the equilibrium between waters inside the pore of the channel and in solution. Because the chemical potential of water in solution decreases as [HCl] increases, it is possible that some of the water molecules inside the channel pore leak out. This would likely result in a major alteration in the water wire structure that could affect or even abolish H^+ transfer and thus g_H. Unfortunately, experimental approaches to probe the chemical potential of waters in the water wire under various experimental conditions have not been successful (see 127).

The magnitude and shape of the log (g_H) – log ($[H^+]$) relationships in the RR channel are different from the SS. Not only is g_H 2-4-fold smaller in the RR than in the SS channel, but a shoulder-type (3) shape in the log (g_H) – log ($[H^+]$) relationship is present in the RR channel. As with the SS channel, saturation of g_H occurs at high [HCl].

The log (g_H) – log ($[H^+]$) relationship in native gA channels is also unique and shares some characteristics of both the RR and the SS channels. While the values of g_Hs are closer to those in the SS channel, the shape of the log-log plot is similar to the one for the RR channel. Interestingly, while there is also saturation of g_H at high $[H^+]$ in native gA channels, these values are closer to 3000 pS. This is significantly larger than in the SS channel (~2000 pS, see above). Consequently, g_H values in gA channels in high [HCl] seem to be strongly but not solely determined by diffusion limitation in solutions.

Figure 12 also shows the dependence of μ_H on $[H^+]$ for the various gA channels (for calculations, see 30). μ_H in gA channels attains values comparable to those in bulk water at very low $[H^+]$. As $[H^+]$ increases, μ_H decreases considerably faster than in water. Notice that the equivalent mobilities for protons (μ_H) in gA channels were also normalized to the *bulk* $[H^+]$. However, the water wire inside gA channels cannot accommodate any number of protons (see 8.5). There is a limit to the number of monovalent cations that can simultaneously occupy a gA channel (2,3,59,95-97). As $[H^+]$ increases, so does the probability of channel occupancy by protons, but *not* the number of excess protons (1 or 2) residing in the channel at any given time. It is possible that the faster decay of μ_H in the various gA channels in relation to water ($[H^+]$ range of 0.001 – 1 M) is a consequence of the stabilization or binding of protons ($(H_3O)^+$, $(H_5O_2)^+$) inside the channel. However, and this point will be revisited later in the review, it is also possible that the faster decline in μ_H – $[H^+]$ for gA channels is a consequence of attenuation of proton transfer in waters at the membrane-channel/solution interface. The structure of waters at these interfaces is different from those in bulk water (48,65,66,98,99), and the rate of proton transfer in those regions may have a different dependency to $[H^+]$ compared to the bulk solution.

In summary, H^+ transfer in water wires inside gA channels in GMO/decane bilayers is highly sensitive to 'simple' modifications of the structure in the middle of the channels. This affects g_H by modifying the interaction between the protonated water chain and channel wall, and as such the residence time of an excess proton inside the channel. Moreover, the series or access resistance that a H^+ must overcome in order to entry or exit the channel is also significant, and seems to account for the saturation and decline of g_H at high [HCl]. The most challenging questions concern the atomic details of the mechanisms underlying those effects, and to what extent the modifications in the middle of the structure of the various gA channels remain localized. In sections 8.3-8.6 below a few quantitative considerations will be made regarding the plots shown in figure 11.

8.3. The thickness of monoglyceride bilayers modulates the transfer of H^+ in gA channels

The experimental measurements of I_H discussed above were obtained in GMO/decane bilayers. The average thickness of these bilayers is 48 Å, and the hydrophobic length of gA channels is ~22 Å. In order for a gA channel to be functional in a bilayer with an average hydrophobic thickness larger than 22 Å, the membrane around the openings of a gA channel must adopt a conformation in which the openings of the channels are exposed to the outside solutions at the same time that the hydrophobic side chain residues of gA are properly shielded by the core of the bilayer (2,80,100-110). Figure 13 is a simple diagram illustrating the basic geometrical relationship between thick or thin bilayers and a gA channel. Notice that in order to have a functional transmembrane gA channel, the thick bilayer has to deform appreciably around the mouths of the channel. In a thin bilayer however, the gA channel can be accommodated without a significant distortion of the

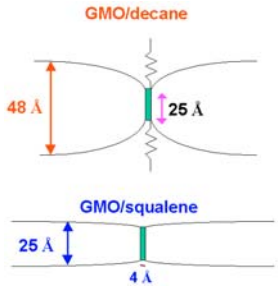

Figure 13. Cartoons of gA channel in thick and thin bilayers, Notice that the funnel shape of the thick bilayer around the opening of the channel is associated with an access resistance to protons. These deformations are less pronounced in thin bilayers.bilayer around the channel. At this point, the dynamics of the lipid bilayer is being neglected, and this issue will be briefly discussed in section 11.1.

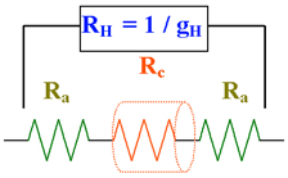

Figure 14. Electrical representation of the access (R_A) and channel (R_C) resistances to proton transfer or diffusion.

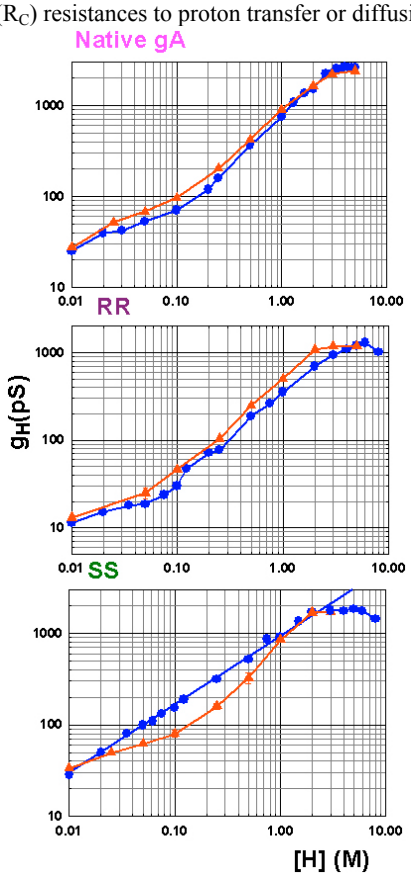

Figure 15. Log-log plots of g_H versus $[H^+]$ for various gA channels in a 48 Å (blue circles), and 28 Å (red triangles) monoglyceride bilayers (from reference 94 with permission).

It has been demonstrated that the thickness of monoglyceride bilayers is determined by a combination of: a) the length of the fatty acid chain; and, b) the solvent used to form the bilayer (76, 111-119). We have found that proton transfer in gA channels is significantly modulated by the thickness of monoglyceride bilayers. g_H values do indeed reflect the total conductance to protons between the two Ag/AgCl electrodes immersed in distinct compartments across the membrane (see figure 5, and the previous section). There are experimental evidences indicating that g_H is comprised components located inside and outside gA channels (see 8.3). A simple equivalent circuit for the total resistance to proton current (R_H) across the membrane is illustrated in figure 14. In this figure, R_A and R_C are the access and channel resistances to proton flow, respectively. Note that $R_H = 1/g_H = (2 \cdot R_A + R_C)$. Because R_C is comparable to the resistance to H^+ flow in bulk water (120), R_A cannot be neglected in determining I_H across gA channels. R_A itself can be decomposed into at least two parts: a) one is the resistance to H^+ flow in bulk solution (see 8.2 above), and, b) another component related to the resistance to H^+ transfer at the membrane-channel/solution interface. The organization of water molecules adjacent to an hydrophobic interface is different from that in bulk solution (48,98,99,121 and references therein). A consequence of this phenomenon was addressed recently by Chiu et al. (65,66) who modeled the diffusion of waters through a native gA channels in a bilayer. These authors calculated that ~90% of the resistance to H_2O diffusion across the gA channel is actually due to very thin regions (~8 Å in width) at the channel-membrane/solution interfaces, and not in the channel itself. The diffusion coefficient of H_2O inside the gA channel is about the same as in bulk solution. It is likely that the properties of H^+ transfer in bulk solution and at the membrane-channel/solution interface are also distinct.

Figure 15 shows log (g_H) – log ($[H^+]$) relationships for the native gA (top panel), RR (middle panel), and SS (bottom panel) channels (94). In each graph, the experimental points were obtained in 'thick' (GMO/decane, 48 Å, blue circles) or 'thin' (GMP(Δ 9 *cis* monopalmitolein)/hexadecane, 28 Å, red triangles) bilayers. GMO and GMP have 18 and 16 carbon fatty acid chains, respectively.

g_H values in native gA or RR channels are consistently larger in thin bilayers at $[H^+]$ <1-2 M. The shapes of the log-log plots are however similar in bilayers of various thicknesses (94). In concentrated solutions of [HCl], g_H values in a given gA channel in bilayers with various thicknesses are similar. The experimental results for the RR and native gA channels are consistent with the possibility that the deformation of the thick bilayer around the mouths of these channels creates a restricted diffusional space that hampers the transfer of protons in and out of the channel. This leads to an increase in R_A in relation to a thin bilayer (see figures 13 and 14). A molecular interpretation for this phenomenon can be attempted if we consider that the opening of gA channels is ~ 4 Å wide. In this case, the narrowest section of the funnel formed by a thick bilayer around a gA channel is ~ 4 Å wide (figure 13, upper

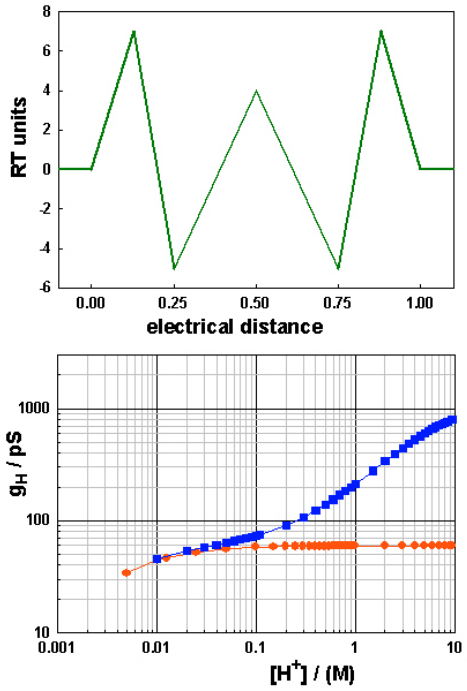

Figure 16. The upper panel shows the energy profile for proton transfer in a gA channel in RT units. The bottom panel shows log-log plots for g_H - $[H^+]$ calculated from the above profile. See text for details.

diagram). Consequently, a single unidimensional file of water molecules should be present in series with gA channels. It is likely that -OH groups from monoglycerides will protrude into that narrow space and establish H-bonds with water molecules. This could result in stabilization of water molecules in those regions. Consequently, the reorientation step of those waters in a Grotthuss mechanism for H^+ transfer would be hampered (R_A increases).

The most interesting and intriguing effect of the thickness of monoglyceride bilayers on g_H was found in the SS channels. In bilayers whose thicknesses are larger than ~ 37 Å, there is a linear relationship (slopes are considerably smaller than 1.00) between log (g_H) and – log ($[H^+]$) (see figure 11 for example). However, in thin (<37 Å) monoglyceride bilayers the log (g_H) – log ($[H^+]$) relationships for the SS channel have a shape similar to those obtained for the native gA or RR channels (see figure 13, bottom panel). These differences in shape are caused by a significant increase in g_H at $0.01 < H^+ < 1$ M. In fact, g_H values in the SS channel approach those measured in native gA channels in that $[H^+]$ range (figure 13). It is possible that the increase in g_H values in the SS channel in thick bilayers is caused by a significant decrease in H^+ (or protonated water cluster) binding inside the SS channel thus increasing H^+ transfer.

How can the differential effects of bilayer thickness on the log (g_H) and – log ($[H^+]$) plots in SS and RR channels be explained? The presence of the dioxolane by itself cannot explain those distinct effects. Perhaps, the rate limiting steps for H^+ transfer *inside* the RR and SS channels are not the same physical process, and the bilayer thickness affects only that rate limiting step in the SS channel. It has been assumed that structural differences between the SS and RR channels are restricted to the region in the middle of the channels (40,77,78). Is it possible that the interactions between the core of the bilayer and the middle regions of gA channels account for the differences in H^+ transfer between the dioxolane-linked gAs? While the mechanisms modulating the linear versus non-linear behavior of (g_H)-$[H^+]$ plots are not yet understood either for a given gA channel in various bilayers or for various gA channels in a given type of bilayer, at least an experimental parameter, the bilayer thickness seems to determine the transition from a linear to a non-linear relationship in the log (g_H) and – log ($[H^+]$) plots for the SS channel. Evidently, the real question concerns the atomic interactions behind this phenomenon.

8.4. Kinetic models of ion permeation inside channels

One way to rationalize the relationships between g_H and $[H^+]$ in water wires in proteins is illustrated in figure 16 (top panel). In the upper graph of this figure, the Gibbs free energy of activation (in RT units) for H^+ transfer in the channel is plotted against the fraction of the applied transmembrane electric field along the water wire inside the pore (electrical distance). The electrical distance is the fraction of the transmembrane voltage that influences a given kinetic step. The positions and ΔG values of peaks and wells are arbitrary. However, the positions and energies of the peaks and wells must be in consonance with the structural symmetry of a gA channel. The bottom graph in figure 16 (red symbols) shows the log-log relationship for a water wire that accepts at most only one proton at any given time (single-occupancy condition). In these simulations, single channel H^+ conductances (pS) were calculated at 10 mV. The plot with red symbols is an adsorption isotherm in which the binding constant of protons to channel relates to the depths of the channel's wells. The blue symbols represent a condition is which two H^+ are allowed to occupy the water wire inside the channel simultaneously. Once this happens, a significant electrostatic repulsion between protons in the water wire occurs. To account for this effect, the rate constant for proton exit from a doubly occupied channel is enhanced 20-fold in relation to the rate constant of a channel that is occupied by a single H^+. Likewise, the entrance rate for a second proton in the channel is slowed down by 20-fold in relation to the entrance rate of a proton in an unoccupied channel. The microscopic reversibility condition was followed in all simulations. This enhancement (or reduction) in rate constants is also arbitrary. However, these changes in the values of rate constants are within the range of electrostatic energies of interaction between two protons in a water wire. In the double occupancy mode, the shape of the log-log plot departs significantly from the graph on the left. Notice that using the same energy profile as in the single occupancy mode, the double occupancy of the pore by H^+ causes a dramatic increase in the rate of proton transfer, mainly at high $[H^+]$.

The experimental measurements of H^+ transfer in various gA channels (like native gA or RR channels in various monoglyceride bilayers, and the SS in *thin* monoglyceride bilayers only) have a shape similar to the plot with blue symbols. Thus, it is conceivable that H^+ transfer under those experimental conditions could occur by a kinetic mechanism involving multiple occupancy of the channel by protons (3,122). Considering that in the simplest case of a symmetrical gA channel there are 6 different parameters (2 energy peaks and 1 energy well, 2 electrical distances, and 1 electrostatic term for repulsion between protons) that can be arbitrarily modified to reproduce the experimental points, it may be possible (even though we have not yet succeeded thus far) to mimic our experimental results using a *formal* kinetic treatments similar to the one in figure 16. However, the linear log-log plots with a slope of ~0.75 for the SS channel in thick bilayers could not be reproduced with the approach illustrated in figure 16.

The modeling used in figure 16 was originally introduced to ion permeation in channels by Eyring et al. (123) and Hille and Schwarz (124). In addition to being a formal and general kinetic treatment, the use of Eyring-rate theory based approaches is questionable and not justifiable conceptually (the interested reader should consult an excellent discussion in several letters sent to the Editor of The Journal of General Physiology, volume 113, June 1999). Perhaps the main virtue of these models is to provide some general conceptual or semi-quantitative guidance to reason about the transfer of protons in water wires (see the following section).

8.5. Factors other than membrane thickness that modulate g_H - $[H^+]$ relationships

Gowen et al. (122) studied the influence of the Trp residues in native gA channels on proton transfer. The replacement of all four Trp residues by Phe (gM channel) or only one Trp by Phe (gB channel) caused marked effects on log (g_H) and – log ($[H^+]$) relationships. The log-log plots of native gA channels were similar to the ones that were described in figures 11 or 15 for native gA channels (see also 3). In gB channels, the shoulder region was shifted by 0.5 pH units to higher $[H^+]$, and in gM channels the log-log relationship became linear within $0.002 \le [H^+] \le 1$ M. The slope of that line was 1.00. This linearization was caused by a decrease in g_H in the range $0.001 \le [H^+] \le 0.05$ M, and an increased g_H at $0.05 \text{ M} \le [H^+] < 1$ M.

These experimental findings were modeled taking into consideration the following parameters:

1. The potential of the mean force (PMF) for an excess proton inside the channel, and for the reorientation of polarizable (PM6) water molecules was taken from the molecular dynamics work using the force field of CHARMm (43,136). These PMFs were incorporated into a model for proton transfer in gramicidin channels (49,137);

2. Gowen et al. (122) limited their analysis to the low end of $[H^+]$. In this range, gA channels work in a single proton occupancy mode (see figure 16). Fits to the log-log relationships for native gA in that range ($2 < [H^+] < 20$ mM) were achieved by optimizing the entrance and exit rates of proton in and out of the channel. This procedure is justifiable considering that there are no force fields defined for these processes, and it has not been possible to measure or model them (see above);

3. In order to fit the linear log-log plot of gM channels, it was necessary to introduce the following modifications in relation to native gA channels:

3.1. An increase by ~ 3 kcal/mol of the proton energy inside gM channels. This procedure is in consonance with the idea that the dipole moments of a pair of indoles groups in the Trp's stabilize a monovalent cation inside the pore by ~ 0.6 kcal/mol (138,139). By removing the Trps in gA channels (gM channels), a proton inside the channel would be destabilized;
3.2. The exit rate in gM channels was enhanced by 65-fold;
3.3. The entrance rate of protons in gM channels becomes voltage dependent and 3-fold slower than in gA channels.

4. Overall, the linearization of the log-log plots in gM channels is caused by extending the range of $[H^+]$ in which the channel is occupied by, at most, one proton at any time.

The linearization of the log-log plots for the SS channels in thick bilayers occurs at the expense of a significant increase in g_H at low $[H^+]$, and the slope of that relationship is not 1.00. It seems that diverse mechanisms account for the effects of Trp residues and the thickness of monoglyceride bilayers on g_H. It is of interest to notice that Gowen et al.'s results (122) could be fitted by altering the kinetics of proton transfer inside *and* outside the water wire in gA channels.

The experiments described in this section were performed in 'thin' GMO/hexadecane experiments. It would be of interest to evaluate the effects of monoglyceride bilayer thickness on proton transfer in gA channels whose Trp residues had been replaced by Phe.

9. ACTIVATION ENERGIES OF PROTON TRANSFER IN GA CHANNELS

The temperature dependency of g_H was studied in various gA channels in GMO/decane membranes (86). In these bilayers, semi-log plots of g_H versus 1/T for the various gA channels yielded Arrhenius type relationships. The various activation energies for H^+ transfer were analyzed, and those results are summarized in Table I. The Gibbs' free energy of activation (ΔG_o) values for the SS and native gA channels are similar. For the RR channel however, ΔG_o is larger by ~2 kJ/mol. This is not surprising considering that a 3-fold difference between g_H values can be accounted for by differences in ΔG_o for H^+ transfer of ~2.5 kJ/mol. A few important points should be remarked (see 86 for a more complete discussion):

1. ΔGo for H+ transfer in gA channels is significantly larger than in HCl solutions (140);

2. ΔGo for H+ transfer in gA channels are in general smaller than those for the permeation of other monovalent cations in native gA channels;

3. Even though DGo values for the various gA channels are similar, there are considerable differences between the values for DHo (activation enthalpy) and ΔSo (activation entropy). In particular, the activation entropy is considerably larger for the RR than for the SS or native gA channels. This accounts for the most part for a smaller gH in RR channels. H+ transfer should be sensitive to the number of possible conformations of the structure of the water wire inside proteins. It is possible that the water wire in RR channels adopts various conformations and some of those cannot transfer H+ or do so with a reduced rate. This would reflect in an increased activation entropy for H+ transfer in the RR channel compared to the SS or native gA channels (see also 40);

4. ΔGo values are nearly the same for the SS and gA channels. However, values for both the ΔHo and ΔSo in these channels are not. There must be considerable fluctuations between the two gA monomers in native gA channels in GMO/decane (thick) bilayers. Because both gA monomers are covalently linked in the SS channel, the fluctuations in the middle of the channel will be constrained or considerably minimized. It is possible that some of these conformations (due to fluctuations) between the gA monomers in native gA channels hamper proton transfer. This could explain the differences between DSo values in the SS and native gA channels. On the other hand, the increased activation enthalpy for the SS in relation to native gA channels could be accounted for by an increased stabilization of a protonated water in the middle of the SS channel due to the presence of a negative electric field created by the oxygens of the dioxolane linker.

An insightful computational study on the influence of the radius of an hydrophobic channel pore on proton transfer in the water wire has demonstrated that when the aqueous environment with an excess proton is sufficiently constrained, there is a significant increase in the mobility of protons in the water wire (38). The interpretation of this phenomenon as well as the one attempted for some of the experimental observations summarized above point to the entropy of water wires as a significant modulators of proton transfer in gA channels.

For reasons that will be explained in section 12, there is a significant difficulty for comparing the experimental data on proton transfer with the computational studies. The determination of ΔG_o for proton transfer in gA channels offers a unique opportunity to check for the validity of some computational approaches. From the potential of the mean force for the reorientation of the unprotonated chain of water molecules, a relatively large barrier for the reorientation of waters in the middle of the channel was calculated. The peak of this barrier is ~ 16 kJ/mol or 9 kJ/mol with polarizable (PM6) or TIP3P water molecules (Pomès and Roux, 2002). The fact that these figures are not in agreement with our measurements (see Table 1 and 86) is not surprising considering the relative simplicity of the initial stage of computational models for proton transfer in water wires. In particular, the entrance and exit rates of protons from (or to) the interface to (or from) channels have not been studied at all.

10. BLOCKING PROTON TRANSFER: THE EFFECTS OF METHANOL IN GA CHANNELS

Ionic currents in biological channels can be blocked by various ions or molecules. Some of these molecules are quite specific for a given ionic current. The literature on this topic is extremely long and diverse. Channel blockers, in addition of being important tools in physiology and neurosciences, have provided insights on the structure and mechanisms by which ion channels work. No specific blockers of H^+ currents in cell membranes have yet been found (142). In principle, a molecule or cation that partitions between water molecules in a water wire could cause attenuation of I_H by temporarily blocking or decreasing the rate of H^+ transfer.

The effects of alcohols, and methanol in particular, on proton transfer have been studied extensively in bulk solution (29,91,125,143). Some experimental observations suggested that H^+ can be transferred between methanol molecules:

1. as it occurs in water, there is an 'extra'-conductivity to protons in relation to other monovalent cations in methanol as solvent (125);

2. in methanol-water mixtures, the proton conductivity declines as the mole fraction of methanol increases. However, within the methanol mole fraction range of 0.8 – 1.0, there is a significant increase in proton conductivity (29);

3. The kinetic isotope effects (KIE) in pure methanol and methanol/water solutions have been recently measured in our laboratory (85). In 1M HCl in pure methanol, the ratio between the conductivities of solutions (HCl - CH_3OH and DCl - CD_3OD) is 1.15. By contrast in 1 M KCl, the ratio between conductivities of solutions (KCl - CH_3OH and KCl - CD_3OD) is 1.24. The differences between the KIE in HCl and KCl suggest that proton transfer may occur in methanol. However, in methanol/water mixtures the KIE for proton transfer was not different from in water solutions. This suggests that H^+ are transferred *mainly* between water molecules in water-methanol mixtures (34,85).

In the top graph of figure 17, measurements of 1 M HCl conductivity (λ, green symbols) and g_H in the SS channel (red symbols) have been plotted as a function of the concentration of methanol in solution (127). In the bottom graph, these measurements were normalized to the values of λ and g_H in the absence of methanol. g_H is considerably more attenuated than λ by methanol. The line connecting the g_H points is based on a model in which one methanol molecule on average partitions inside the pore of the SS channels and 'blocks' I_H (127).

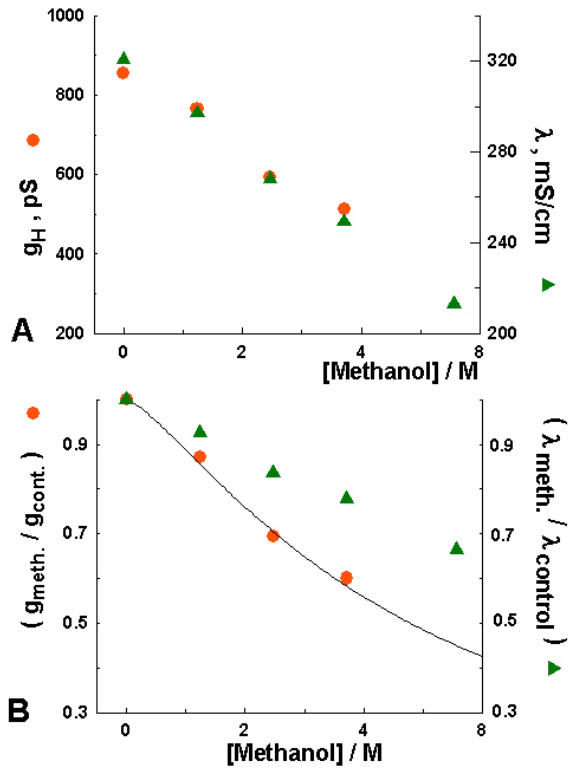

Figure 17. Bulk conductivity of HCl solutions (λ) and g_H in the SS channel as a function of methanol concentration (from reference 127 with permission). Raw measurements are shown in A, and normalized values in B. See text.

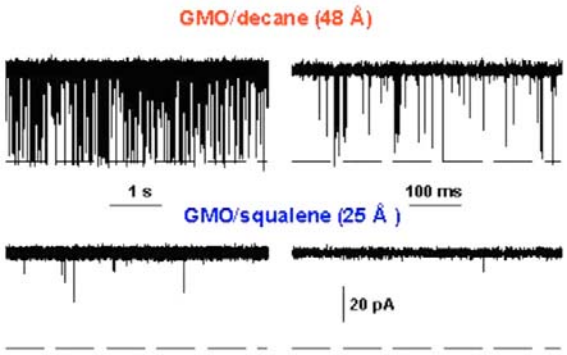

Figure 18. Recordings of single SS channels in 1 M HCl in monoglyceride bilayers of various thicknesses (from reference 80 with permission). Note that recordings on the left and right columns have different time scales.

It is of interest to notice that:

1. the permeation of Cs^+ in various gA channels is not affected by methanol (127; Godoy and Cukierman, unpublished observations);

2. ethanol and propanol are alcohols that would not fit inside the pore of gA channels. Both ethanol and propanol do not attenuate I_H in gA channels (Godoy and Cukierman, unpublished observations);

The basic mechanisms by which methanol attenuates proton transfer in gA channels remains elusive (85,129). It is possible that protons are transferred between water and methanol at a considerably lower rate than between water molecules. Alternatively, methanol does not transfer protons inside the channel at all, and proton transfer inside the channel will be blocked during the permanence of methanol inside the water wire.

11. THE ORIGIN OF THE BRIEF CLOSING EVENTS IN GA CHANNELS

In section 5.1, a description of the short duration closing events (flickers) in native gA channels was given. A recent hypothesis concerning the possible origin of flicker activity will be reviewed here (80).

Submilisecond closures (as shown in figure 9) were previously described for native gA (128,129), RR channels and in SS channels (77). It was also shown for native gA channels only that the frequency of those flickers was considerably attenuated in thin bilayers (128,129). Figure 18 shows I_H recordings of single SS channels in thick (top recording), and thin (bottom recording) GMO membranes. Notice in this figure the two different time scales for the recordings on the right and left columns. The flicker frequency is attenuated by 100-fold in the SS channel in thin bilayers (80). In the bottom recordings of figure 18, there are practically no flickers. Qualitatively similar results were also obtained for the RR and native gA channels (80). It should be noted that a significant number or perhaps the majority of flickers cannot be entirely resolved due to limitations in the bandwidth of the recording system.

gA monomers in the SS and RR channels do not dissociate. Thus, it is not likely that flickers in these covalently linked channels are caused by pre-dissociation or dissociation states that may result from fluctuations between two gA monomers in native gA channels. Because a) the flicker frequency is heavily modulated by the thickness of monoglyceride bilayers, and b) it is not likely that side chain residues of gA channels flip inside the pore of gA channels obliterating the water wire, it was proposed that flickers originate from the dynamics of interaction between gA channels and membrane.

The thickness of lipid bilayers must be evaluated from a dynamical point of view (102,103,109). At room temperatures, biological membranes have thermal undulations whose characteristics have been recently measured experimentally (130,131), and can be reproduced in a mesoscopic scale in computer simulations (102,132-134,149). The diameter of the openings of gA channels is ~ 4Å, and bilayer undulations can be large enough (130,131) to partially or completely obliterate the vestibules that develop in thick bilayers and connect the openings of gA channels to the solutions outside the channel. A cartoon of a channel-membrane is shown in figure 19. Notice that in the 'thick' bilayer (top diagram) the presence of undulations obliterate the openings of the channel. In thin bilayers however, there would be a relatively small

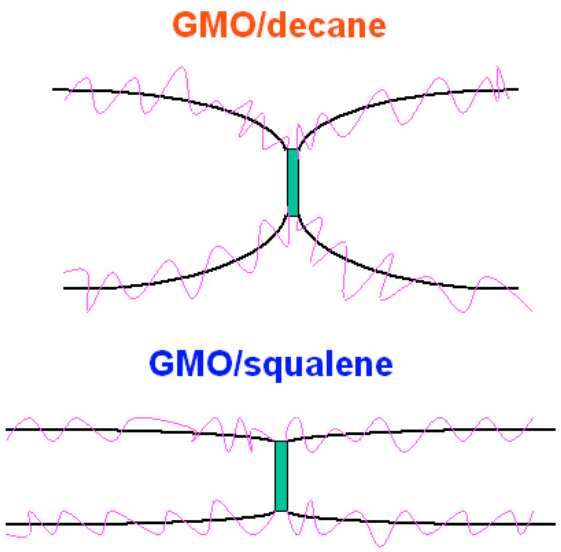

Figure 19. Cartoons illustrating the possible effects of bilayer undulations on closing flickers in gA channels. The black thick line illustrates the 'average' thickness of the lipid bilayer. Superimposed on this average thickness, are free-hand drawings (pink lines) of bilayer undulations. See text for discussion.

deformation of the membrane adjacent to the channel openings, and the frequency of undulations that could obstruct the channel mouth should be relatively smaller compared to thick bilayers. Such a mechanism could explain the dramatic attenuation of flicker frequency in thin bilayers (80). However, experimental observations that remain to be explained regard differences in flicker frequencies between native gA, SS, and RR channels in thick and thin bilayers (80). Is it possible that modifications in the middle of the channel can modulate the interactions between membrane and channel at the bilayer surface?

12. SUMMARY AND PERSPECTIVES

It has been known for a long time that g_H in native gA channels is quite large compared to the single channel conductances of other monovalent cations (1-3). It had also been proposed, in analogy with what was already known for water, that this large g_H is caused by a special transfer mechanism for protons that might be occurring in native gA channels (1,2). Only recently however, was this large g_H rediscovered and analyzed in more detail having in mind the conceptual framework of a water wire and the perspective of bioenergetic proteins (31,37,84). Akeson and Deamer (84) measured the kinetic isotope effects for H^+ permeation in native gA channels and found a value consistent with proton transfer. Our laboratory has demonstrated that in the dioxolane-linked gA channels protons are transferred. This transfer is modulated by various factors including the stereochemistry of the dioxolane, the nature of the lipid bilayer, and the access resistances to proton entry and exit in the channels (30,78,80-82,85-87,94,120,127,144). The activation energies of proton transfer in these channels were also measured (86). Busath, Cross, Schumaker and collaborators have studied the influence of the Trp residues, or their dipole moments, in native gA channels on proton transfer (49,122,137-139). Antonenko and colleagues have investigated the role of the membrane dipole potential on g_H (145). Most of these studies were published in the last few years only. gA channels constitute an interesting model to probe proton transfer in water wires inside protein cavities. Today we definitely know more about proton wires than we did just a few years ago, and, most importantly, we have specific questions to address. However, a clear atomistic picture of the rate limiting steps of proton transfer in water wires inside these proteins is still absent. Thus, it is not known how modulation of proton transfer by the various factors discussed in this review occurs. Evidently, one of the challenges is to understand the experimental observations from the mechanistic point of view of molecular dynamics.

Even though this review has focused mostly on the experimental measurements of proton transfer, there has also been a recent rediscovery of proton transfer mechanisms using computational and theoretical methods to study water wires (28-40,43-47,49,136). As with the experimental measurements of proton transfer in well-defined systems, a considerable progress has occurred in recent years using molecular dynamics simulations. Because of computer limitations, simulations can be performed up to a few nanoseconds only, and using models that oversimplify the complex biophysical reality. Thus, it has not been possible to correlate the findings of these interesting and necessary computational studies with actual experimental measurements (see for example section 9). Some difficulties can be identified: a) the short time interval of the computer simulations; b) the absence of a lipid bilayer, and of bulk and interface solutions that mimic the extra-channel aqueous environments across the membrane; c) proton transfer at membrane-channel/solutions interfaces has not been addressed; d) the implicit assumptions and uncertainties regarding molecular dynamics simulations including the incompleteness of available force fields (146,147) and the lack of an appropriate model for water molecules (see section 9, and 148); e) the absence of an electrochemical gradient across the membrane. It would also be instructive to investigate the properties of water wires with two excess protons instead of only one. For the sake of fairness, it should be remarked that a significant number of computational studies predated the development of the experimental work reviewed here on H^+ transfer. Hopefully, these two essential lines of investigation will benefit directly from each other in the future.

Some recent technological developments (148) will hopefully extend the time resolution of single channel currents to levels shorter than presently possible. In particular, this will be extremely useful for studying closing flickers. As computers and algorithms become more powerful it will be possible to narrow the gap between the timeframes of experimental measurements and molecular dynamics simulations. It should also be mentioned that Schumaker and collaborators developed a creative

mathematical framework that extends the MD simulations to the level of measured single channel currents (49,122,137). It will be of interest to verify if the application of this framework to 'improved' force fields reproduces the measurable proton transfer in gA channels. This may have profound implications for the study of ion permeation in ion channels in general.

Recent MD studies were performed with ion channels imbedded in a lipid membrane with solutions. Still there are some essential conceptual problems that were not or have been difficult to address like the behavior of channel-membrane/solution interfaces. MD is an extremely powerful method. We are unable to see molecules or groups of atoms in action in real time, and MD offers this virtual opportunity that is extremely important for the formulation of hypothesis and the development of new and original experimental approaches.

13. ACKNOWLEDGMENTS

I am thankful to NIH (GM 50674) for the steadfast support. Many thanks to Kathryn M. Armstrong, Anatoly Chernyshev, David S. Crumrine, April Emerick, Carlos Marcelo de Godoy, Edward P. Quigley, and Shasikala Narayan for discussions.

14. REFERENCES

1. Myers V.B., and D.A Haydon. Ion transfer across lipid membranes in the presence of gramicidin A. *Biochem. Biophys. Acta* 274, 313-322 (1972)

2. Hladky S.B., and D.A. Haydon. Ion transfer across lipid membranes in the presence of gramicidin A. I. Studies of the unit conductance channel. *Biochem. Biophys. Acta* 274, 294-312 (1972)

3. Eisenman G., B. Enos, J. Hägglund, and J. Sandblom. Gramicidin A as an example of a single filing ionic channel. *Ann. N.Y. Acad. Sci.* 329,8-20 (1980)

4. Bell R.P. The Proton in Chemistry. Cornell University Press (1959)

5. DeCoursey T.E. Hypothesis, do voltage-gated H^+ channels in alveolar epithelial cells contribute to CO_2 elimination by the lung? Am. J. Physiol. Cell Physiol. 278, C1-C10 (2000)

6. DeCoursey, T.E., V.V. Cherny, W. Zhou, and L. L. Thomas. Simultaneous activation of NADPH oxidase-related proton and electron currents in human neutrophils. *Proc. Natl. Acad. Sci. USA* 97, 6885-6889 (2000)

7. Tu C., M. Qian, J. N. Earnhardt, P. J. Laipis, and D. N. Silverman. Properties of intramolecular proton transfer in carbonic anhydrase III. Biophys. J. 74, 3182-3189 (1998)

8. Macnab R.M. The bacterial flagellum, reversible rotary propellor and type III export apparatus. *J. Bacteriol.* 181, 7149-7153 (1999)

9. Nelson N., and W.R. Harvey. Vacuolar and plasma membrane proton-adenosinetriphosphatases. Physiol. Rev. 79, 361-385 (1999)

10. Dschida W.J., and B. J. Bowman. Structure of the vacuolar ATPase from *Neurospora crassa* as determined by electron microscopy. *J. Biol. Chem*. 267, 18783-18789 (1992)

11. Boekema E.J., J. F. van Breemen, A. Brisson, T. Ubbink-Kok, W. N. Konings, and J. S. Lolkena. Connecting stalks in V-ATPase. Nature 401, 37-38 (1999)

12. Forgac M. Structure and properties of the vacuolar (H^+)-ATPase. J. Biol. Chem. 274, 12951-12954 (1999)

13. Alberts B., D. Bray, J. Lewis, M. Raff, K. Roberts, and J.D. Watson. Molecular Biology of the Cell. 3rd. Edition, Garland Publishing, New York (1994)

14. Baciou, L., and H. Michel. Interruption of the water chain in the reaction center from *rb. sphaeroides* reduces the rate of the proton uptake and of the second electron transfer to Q_B. *Biochem.* 34, 7967-7972 (1995)

15. Tandori J., P. Sebban, H. Michel, and L. Baciou. In *Rhodobacter sphaeroides* reaction centers, mutation of proline L209 to aromatic residues in the vicinity of a water channel alters the dynamic coupling between electron and proton transfer processes. *Biochem.* 38, 13179-13187 (1999)

16. Abramson J., M. Ek-Svensson, B. Byrne, and S. Iwata. Structure of cytochrome *c* oxidase, a comparison of the bacterial and mitochondrial enzymes. *Biochem. Biophys. Acta* 1544, 1-9 (2001)

17. Branden M., H. Sigurdson, A. Namslauer, R. B. Gennis, P. Adelroth, and P. Brzezinski. On the role of the K-proton transfer pathway in cytochrome *c* oxidase. *Proc. Natl. Acad. Sci. USA* 98, 5013-5018 (2001)

18. Iwata S., C. Ostermeier, B. Ludwig, and H. Michel. Structure at 2.8 Å resolution of cytochrome *c* oxidase from *Paracoccus denitrificans*. Nature 376, 660-669 (1995)

19. Tsukihara T., H. Ayoama, E. Yamashita, T. Tomiza, H. Yamagushi, K. Shinzawa-Itoh, R. Nakajima, R. Yaono, and S. Yoshikawa. The whole structure of the 13-subunit oxidized cytochrome *c* oxidase at 2.8 Å. Science 272, 1136-1144 (1996)

20. Zaslavsky D., and R. B. Gennis. Substitution of lysine-362 in a putative proton-conducting channel in the cytochrome *c* oxidase from *Rhodobacter sphaeroides* blocks turnover with O_2 but not with H_2O_2. *Biochem.* 37, 3062-3067 (1998)

21. Zaslavsky D., and R. B. Gennis. Proton pumping by cytochrome oxidase, progress, problems, and postulates. Biochim. Biophys. Acta 1458, 164-179 (2000)

22. Luecke H., B. Schobert, H.T. Richter, J. P. Cartailler, and J. K. Lanyi. Structure of bacteriorhodopsin at 1.55 Å resolution. *J. Mol. Biol.* 291, 899-911 (1999)

23. Martinez, S.E., D. Huang, M. Ponomarev, W.A. Cramer, and J.L. Smith. The heme redox center of chloroplast cytochrome *f* in linked to a buried 5-water chain. *Protein Sci.* 5,1081-1092 (1996)

24. Rastogi V. K., and M. E. Girvin. Structural changes linked to proton translocation by subunit *c* of the ATP synthase. Nature 402, 263-268 (1999)

25. Adams M.W.W., and E.I. Stiefel. Biological hydrogen production, not so elementary. *Science* 282, 1842-1843 (1998)

26. Peters J.W., W. N. Lanzilotta, B.J. Lemon, and L.C. Seefeldt. X-ray crystal structure of the Fe-only hydrogenase (Cpl) from *Clostridium pasteurianum* to 1.8 Å angstrom resolution. *Science* 282, 1853-1858 (1998)

27. Danneel V.H. Notiz über ionengeschwindigkeiten. *Z. Elektrochem.* 11, 249-252 (1905)

28. Bernal J.D., and R. H. Fowler. A theory of water and ionic solution, with particular reference to hydrogen and hydroxyl ions. *J. Chem. Phys.* 1, 515-548 (1993)

29. Conway B.E., J.O.M. Bockris, and H. Linton. Proton conductance and the existence of the H_3O^+ ion. *J. Chem. Phys.* 24, 834- 852 (1956)

30. Cukierman S. Proton mobilities in water and in different stereoisomers of covalently linked gramicidin A channels. *Biophys. J.* 78, 1825-1834 (2000)

31. Nagle J.F., and S. Tristam-Nagle. Hydrogen bonded chain mechanisms for proton conduction and proton pumping. *J. Memb. Biol.* 74, 1-14 (1983)

32. Agmon, N. Hydrogen bonds, water rotation and proton mobility. *J.Chim.Phys.* 93, 1714-1736 (1996)

33. Agmon, N. Proton solvation and proton mobility. *Isr. J. Chem.* 39, 493-502 (1999)

34. Agmon, N. The Grotthuss Mechanism. *Chem. Phys. Lett.* 244, 456-462 (1995)

35. Day T.J.F., U.W. Schmitt, and G.A. Voth. The mechanism of hydrated proton transfer in water. *J. Am. Chem. Soc*. 122,12027-12028 (2000)

36. Tuckerman M., K. Laasonen, M. Sprik, and M. Parinello. *Ab initio* molecular dynamics simulation of the solvation and transport of H_3O^+ and OH^- ions in water. *J. Phys. Chem.* 99, 5749-5752 (1995)

37. Nagle J.F., and H.J. Morowitz. Molecular mechanisms for proton transport in membranes. *Proc. Natl. Acad. Sci. USA* 75, 298-302 (1978)

38. Brewer M.L., U.W. Schmitt, and G.A. Voth. The formation and dynamics of proton wires in channel environment. *Biophys. J.* 80,1691-1702 (2001)

39. Yu C.H., S. Cukierman, and R. Pomès. Structure and fluctuations of water wires in dioxolane-linked gramicidin channels. Biophys. J. 82, 209a (2002a).

40. Yu C.H., S. Cukierman, and R. Pomès. Theoretical study of the structure and dynamic fluctuations of dioxolane-linked gramicidin channels. Biophys. J. (2002b)

41. DeCornez H., K. Drukker, and S. Hammes-Schiffer. Solvation and hydrogen-bonding effects on proton wires. J. Phys. Chem. A. 103, 2891-2898 (1999)

42. Marrink S.J., F. Jähnig, and H.J.C. Berendsen. Proton transport across transient single-file water pores in a lipid membrane studied by molecular dynamics simulations. *Biophys. J.* 71, 632-647 (1996)

43. Pomès R., and B. Roux. Structure and dynamics of a proton wire, a theoretical study of H^+ translocation along the single-file water chain in the gramicidin A channel. *Biophys. J.* 71, 19-39 (1996)

44. Pomès R., and B. Roux. Free energy profiles for H^+ conduction along hydrogen-bonded chains of water molecules. *Biophys. J.* 75, 33-40 (1998)

45. Pomès R. Theoretical studies of the Grotthuss mechanism in biological proton wires. *Isr. J. Chem.* 39, 387-395 (1999)

46. Sagnella D.E., and G.A. Voth. Structure and dynamics of hydronium in the ion channel gramicidin A. *Biophys. J.* 70, 2043-2051 (1996)

47. Sagnella D.E., K. Laasonen, and M. Klein. Ab-initio molecular dynamic study of proton transfer in a polyglycine analog of the ion channel gramicidin A. *Biophys. J.* 71,1172-1178 (1996)

48. Sansom M.S.P., I.D. Kerr, J. Breed, R. Sankararamakrishnan. Water in channel-like cavities, structure and dynamics. *Biophys. J.* 70,693-702 (1996)

49. Schumaker, M.F., R. Pomès, and B. Roux. A combined molecular dynamics and diffusion model of single proton conduction through gramicidin. *Biophys. J.* 79, 2840-2857 (2000)

50. Trumpower B.L., R. B. Gennis. Energy transduction by cytochrome complexes in mitochondrial and bacterial respiration, the enzymology of coupling electron transfer reactions to transmembrane proton translocation. *Ann. Rev. Biochem.* 63, 675-716 (1994)

51. Arseniev A.S., I.L. Barsukov, V.F. Bystrov, AL. Lonize, and Y.A. Ovchinikov. Proton NMR study of gramicidin A transmembrane ion channel. Head-to-head right handed, single stranded helices. *FEBS Lett.* 186, 168-174 (1985)

52. Ketchem R.R., B. Roux, and T.A. Cross. High-resolution polypeptide structure in a lamellar phase lipid environment from solid state NMR derived constraints. *Structure* 5,1655-1669 (1997)

53. Ketchem R.R., W. Hu, and T.A. Cross. High resolution of gramicidin A in a lipid bilayer by solid-state NMR. *Science* 261, 1457-1460 (1993)

54. Sarges R., and B. Witkop. V. The structure of valine- and isoleucine-gramicidin A. *J. Am. Chem. Soc.* 87, 2011-2019 (1965)

55. Urry D.W. Gramicidin A transmembrane channel, a proposed $\pi_{(L,D)}$ helix. *Proc. Nat. Acad. Sci.* USA 68, 672-676 (1971)

56. Andersen, O.S. Gramicidin channels. *Ann. Rev. Physiol.* 46, 531-548 (1984)

57. Koeppe II, R.E., and O.S. Andersen. Engineering the gramicidin channel. *Annu. Rev. Biophys. Biomol. Struct.* 25, 231-258 (1996)

58. Hladky S.B., and D.A. Haydon. Ion movements in gramicidin channels. *Curr. Top. Membr. Transp.* 21, 327-372 (1984)

59. Finkelstein A., and O.S. Andersen. The gramicidin A channel, a review of its permeability characteristics with special reference to the single-file aspect of transport. *J. Memb. Biol.* 39, 155-171 (1981)

60. Finkelstein A. Water movement through lipid bilayers, pores, and plasma membrane. Theory and Reality. John Willey, New York (1987)

61. Levitt D.G. Kinetics of movement in narrow channels. *Curr. Topics in Memb. and Transp.* 21, 181- 197 (1984)

62. Levitt D.G., S.R. Elias, and J.M. Hautman. Number of water molecules coupled to the transport of sodium, potassium, and hydrogen ions via gramicidin nonactin or valinomycin. *Biochem. Biophys. Acta* 512, 436-451 (1978)

63. Rosenberg P.A., and A. Finkelstein. Interaction of ions and water in gramicidin A channels. Streaming potentials across lipid bilayer membranes. *J. Gen. Physiol.* 72, 327-340 (1978)

64. Tripathi S., and S.B. Hladky. Streaming potentials in gramicidin channels measured with ion selective electrodes. Biophys. J. 74, 2912-2917 (1998)

65. Chiu S.W., S. Subramanian, and E. Jakobsson. Simulation study of a gramicidin/lipid bilayer system in excess water and lipid. I. Structure of the molecular complex. *Biophys. J.* 76, 1929-1938 (1999)

66. Chiu S.W., S. Subramanian, and E. Jakobsson. Simulation study of a gramicidin/lipid bilayer system in excess water and lipid. II. Rates and mechanisms of water transport. *Biophys. J.* 76, 1939-1950 (1999)

67. De Groot B.L, D.P. Tieleman, P. Pohl, and H. Grubmüller. Water permeation through gramicidin A, desformylation and the double helix, a molecular dynamics study. *Biophys. J.* 82, 2934-2942 (2002)

68. Jordan, P.C. Ion-water and ion-polypeptide correlations in a gramicidin-like channel. A molecular dynamics study. *Biophys. J.* 58,1133-1156 (1990)

69. Lee W.K., and P.C. Jordan. Molecular dynamics simulation of cation motion in water-filled gramicidinlike pores. *Biophys. J.* 46, 805-819 (1984)

70. Mackay D.H.J., P.H. Berens, K.R. Wilson. Structure and dynamics of ion transport through gramicidin A. *Biophys. J.* 46, 229-248 (1984).

71. Woolf T. B., and B. Roux. Structure, energetics, and dynamics of lipid-protein interactions, a molecular dynamics study of the gramicidin A channel in DMPC bilayer. *Proteins* 24, 92-114 (1996)

72. Urry D.W., M.C. Goodall, J.D. Glickson, and D.F. Meyers. The gramicidin A transmembrane channel: characteristics of head-to-head dimerized $\pi_{(L,D)}$ helices. *Proc. Nat. Acad. Sci. USA* 68, 1907-1911 (1971)

73. Andersen O.S., H.J. Apell, E. Bamberg, D.D. Busath, R.E. Koeppe II, F.J. Sigworth, G. Szabo, D.W. Urry, and A. Wooley. Gramicidin channel controversy – the structure in a lipid environment. *Nature Struct. Biol.* 6, 609 (1999)

74. Burkhart B.M., and W.L. Duax. Gramicidin channel controversy- reply. *Nature Struct. Biol.* 6, 611-612 (1999)

75. Bamberg E., and K. Janko. The action of a carbonsuboxide dimerized gramicidin A on lipid bilayer membranes. *Biochem. Biophys. Acta* 465, 486-499 (1977)

76. Rudnev V.S., L.N. Ermishkin, L.A. Fonina, and Yu. G. Rovin. The dependence of the conductance and lifetime of gramicidin channels on the thickness and tension of lipid bilayers. *Bioch. Biophys. Acta* 642, 196-202 (1981)

77. Stankovic, C.J., S.H. Heinemann, J.M. Delfino, F.J. Sigworth, and S.L. Schreiber. Transmembrane channels based on tartaric acid-gramicidin A hybrids. *Science* 244, 813-817 (1989)

78. Quigley E.P., P. Quigley, D.S. Crumrine, and S. Cukierman. The conduction of protons in different stereoisomers of dioxolane-linked gramicidin A channels. *Biophys. J.* 77, 2479-2491 (1999)

79. Crouzy S., T.B. Woolf, and B. Roux. A molecular dynamics study of gating in dioxolane-linked gramicidin A channels. *Biophys. J.* 67, 1370-1386 (1994)

80. Armstrong K.M., and S. Cukierman. On the origin of closing flickers in gramicidin channels, a new hypothesis. *Biophys. J.* 82, 1329-1337 (2002)

81. Armstrong K.M., E. P. Quigley, P. Quigley, D. S. Crumrine, and S. Cukierman. Covalently linked gramicidin channels, effects of linker hydrophobicity and alkaline metals on different stereoisomers. *Biophys. J.* 80, 1810-1818 (2001)

82. Quigley E.P., D.S. Crumrine, and S. Cukierman. Gating and permeation in ion channels formed by gramicidin A and its dioxolane-linked dimer in Na^+ and Cs^+ solutions. *J. Memb. Biol.* 174, 207-212 (2000)

83. Tredgold R.H. , R. Jones. A study of gramicidin using deuterium oxide. *Biochim. Biophys. Acta* 550 ,543-545 (1979)

84. Akeson M., and D.W. Deamer. Proton conductance by the gramicidin water wire. Model for proton conductance in the F_0F_1ATPases? *Biophys. J.* 60, 101-109 (1991)

85. Chernyshev A., R. Pomès, and S. Cukierman. Kinetic isotope effects of proton transfer in aqueous and methanol containing solutions, and in gramicidin channels. *Biophys. Chem.* (in press, 2002).

86. Chernyshev A., and S. Cukierman. Thermodynamic view of activation energies of proton transfer in various gramicidin A channels. *Biophys. J.* 82, 182-192 (2000)

87. Godoy C.M.G, and S. Cukierman. Modulation of proton transfer in the water wire of dioxolane-linked gramicidin channels by lipid membranes. *Biophys. J.* 81, 1430-1438 (2001)

88. Eisenberg D., and W. Kauzmann. The structure and properties of water. Oxford University Press, New York (1969)

89. Agmon, N. Structure of concentrated HCl solutions. *J. Phys. Chem.*102, 192-199 (1998)

90. Kameda Y., Usuki T., and O. Uemura. Neutron Diffraction studies on the hydrogen-bonded structure in concentrated aqueous hydrochloric acid solutions. *Bull. Chem. Soc. Jpn.* 71, 1305-1313 (1998)

91. Lengyel S., J. Giber, and J. Tamás. Determination of ionic mobilities in aqueous hydrochloric acid solutions of different concentration at various temperatures. *Acta Chim. Hung.* 32, 429-436 (1962)

92. Lown D.A., and H.R. Thirsk. Proton transfer conduction in aqueous solution. Part 1. Conductance of concentrated aqueous alkali metal hydroxide solutions at elevated temperatures and pressures. *Trans. Faraday Soc.* 67, 132-148 (1971)

93. Owen, B. B., F. H. Sweeton. The conductance of hydrochloric acid in aqueous solutions from 5^o to 65^o. *J. Am. Chem. Soc.* 63, 2811-2817 (1941)

94. Chernyshev A., K.M. Armstrong, and S. Cukierman. Proton transfer in gramicidin channels is modulated by the thickness of monoglyceride bilayers. *Biophys. J.(in press, 2002)*.

95. Doyle D.A., and B.A. Wallace. Crystal structure of the gramicidin/potassium thiocyanate complex. *J. Mol. Biol.* 266,963-977 (1997)

96. Tian F., and T.A. Cross. Cation transport, an example of structural based selectivity. *J. Mol. Biol.* 285, 1993-2003 (1999)

97. Tian F., K.C. Lee, W. Hu, and T.A. Cross. Monovalent cation transport, lack of structural information upon cation binding. *Biochem*. 35, 11959-11966 (1996)

98. Breed J., R. Sankararamakrishnan, I.D. Kerr, and M.S.P. Sansom. Molecular simulations of water within models of ion channels. *Biophys. J.* 70,1643-1661 (1996)

99. Lee W.K., and P.C. Jordan. Molecular dynamics simulation of cation motion in water-filled gramicidinlike pores. *Biophys. J.* 46, 805-819 (1984)

100. De Planque M. R. R., D. V. Greathouse, R. E. Koeppe II, H. Schäfer, D. Marsh, and J. A. Killian. Influence of lipid/peptide hydrophobic mismatch on the thickness of diacylphosphatidylcholine bilayers. A ^{2}H NMR and ESR using designed transmembrane α-helical peptides and gramicidin A. *Biochem.* 37, 9333-9345 (1998)

101. Hendry B.M., B. W. Urban, and D.A. Haydon. The blockage of the electrical conductance in a pore-containing membrane by the n-alkanes. *Biochim. Biophys. Acta* 513, 106-116 (1978)

102. Helfrich P., and E. Jakobsson. Calculation of deformation energies and conformations in lipid membranes containing gramicidin channels. *Biophys. J.* 57, 1075-1084 (1990)

103. Huang H.W. Deformation free energy of bilayer membrane and its effect on gramicidin channel lifetime. *Biophys. J.* 50, 1061-10170 (1986)

104. Elliot J.R., D. Neddham, J. P. Dilger, and D.A. Haydon. The effects of bilayer thickness and tension on gramicidin single-channel lifetime. *Biochim. Biophys. Acta* 735, 95-103 (1983)

105. Killian J.A., de Planque M. R. R., vand der Wel P. C. A., Salemink I., de Kruijff, Greathouse D. V., and Koeppe II, R.E. Modulation of membrane structure and function by hydrophobic mismatch between protein and lipids. *Pure and Appl. Chem.* 70, 75-82 (1998)

106. Kolb H.A., and E. Bamberg. Influence of membrane thickness and ion concentration on the properties of the gramicidin A channel. *Biochim. Biophys. Acta* 464, 127-141 (1977)

107. Lundbæk JA, and O.S. Andersen. Lysophospholipids modulate channel function by altering the mechanical properties of lipid bilayers. *J. Gen. Physiol.* 104, 645-673 (1994)

108. Lundbæk J.A., P. Birn, J. Girshman, A. J. Hanse, and O.S. Andersen. Membrane stiffness and channel function. *Biochem.* 35, 3825-3830 (1996)

109. Ring A. Gramicidin channel-induced lipid membrane deformation energy, influence of chain length and boundary conditions. *Biochim. Biophys. Acta* 1278, 147-159 (1996)

110. Van de Wel P.C.A., T. Pott, S. Morein, D. V. Greathouse, R. Koeppe II, and J.A. Killian. Tryptophan-anchored transmembrane peptides promote formation of nonlamellar phases in phosphatydylethanolamine model membranes in a mismatch-dependent manner. *Biochem.* 39, 3124- 3133.

111. Benz R., O. Frohlich, P. Lauger, and M. Montal. Electrical capacity of black lipid films and of lipid bilayers made from monolayers. *Biochem. Biophys. Acta* 394, 323-334 (1975)

112. Dilger J.P. The thickness of monoolein lipid bilayers as determined from reflectance measurements. *Biochim. Biophys. Acta* 645, 357-363 (1981)

113. Dilger J.P., and R. Benz. Optical and electrical properties of thin monoolein bilayers. *J. Memb. Biol.* 85, 181-189 (1985)

114. Elliot J.R., D. Neddham, J. P. Dilger, and D.A. Haydon. The effects of bilayer thickness and tension on gramicidin single-channel lifetime. *Biochim. Biophys. Acta* 735, 95-103 (1983)

115. Lewis B.A., and D. M. Engelman. Lipid bilayer thickness varies linearly with acyl chain length in fluid phosphatidylcholine vesicles. *J. Mol. Biol.* 166, 211-217 (1983)

116. McIntosh T.J., S. A. Simon, and R. C. MacDonald. The organization of n-alkanes in lipid bilayers. *Biochim. Biophys. Acta.* 597,445-63 (1980)

117. Requena J., D.F. Billett, and D.A. Haydon. Van der Waals forces in oil-water systems from the study of thin lipid films. *Proc. R. Soc. A.* 347, 141-159 (1975)

118. Simon S.A., L.J. Lis, R. C. MacDonald R.C., and J. W. Kauffman. The noneffect of a large linear hydrocarbon, squalene, on the phosphatidylcholine packing structure. *Biophys. J.* 19, 83-90 (1977)

119. White S.H. Formation of 'solvent-free' black lipid bilayer membranes from glyceryl monooleate dispersed in squalene. *Biophys. J.* 33, 337-247 (1978)

120. Cukierman S. Flying protons in linked gramicidin A channels. *Isr. J. Chem*. 39, 419-426 (1999)

121. Israelachvili J.N. Intermolecular and surface forces. Second Edition. Academic Press, London (1992)

122. Gowen J.A., J.C. Markham, S.E. Morrison, T.A. Cross, D.D. Busath, E.J. Mapes, and M.F. Schumaker. The role of Trp side chains in tuning single proton conduction through gramicidin channels. *Biophys. J.* 83, 880-898 (2002)

123. Eyring H., R. Lumry, and J.W. Woodbury. Some applications of modern rate theory to physiological systems. *Rec. Chem. Prog*. 10, 100-114 (1949)

124. Hille B., and W. Schwarz. Potassium channels as multi-ion single-file pores. *J. Gen. Physiol.* 72, 409-442 (1978)

125. Conway B.E. Proton solvation and proton transfer processes in solution. In Modern Aspects of Electrochemistry, Editors, J.O.M. Bockris, and B. E. Conway, London, Butterworths 3, 43- 148 (1964)

126. Agmon N., S.Y. Goldberg, and D. Huppert. Salt effect on transient proton transfer to solvent and microscopic proton mobility. *J. Mol. Liquids* 64, 161-195 (1995)

127. Quigley E.P., A. Emerick, D.S. Crumrine, and S. Cukierman. Proton current attenuation by methanol in a dioxolane-linked gramicidin A dimer in different lipid bilayers. *Biophys. J.* 5, 2811-2820 (1998)

128. Ring A. Brief closures of gramicidin A channels in lipid bilayer membranes. *Biochim. Biophys. Acta* 856, 646-653 (1986)

129. Sigworth F.J., and S. Shenkel. Rapid gating events and current fluctuation in gramicidin A channels. *Curr. Top. Memb. Transp*. 33, 113-130 (1988)

130. Hirn R., T. M. Bayerl, J. O. Radler, and E. Sackmann.. Collective membrane motions of high and low amplitude, studied by dynamic light scattering and micro-interferometry. *Faraday Disc*. 111, 17-30 (1998)

131. Sackmann E. Membrane bending energy concept of vesicle- and cell-shapes and shape-transitions. *FEBS Lett.* 346, 3-16 (1994)

132. Bach D, and I. R. Miller. Glyceryl monooleate black lipid membranes obtained from squalene solutions. *Biophys. J.* 29, 183-188 (1980)

133. Ayton G., A. M. Smondyrev, S.G. Bardenhagen, P. McMurtry, and G.A. Voth. Interfacing molecular dynamics

and macro-scale simulations for lipid bilayer vesicles. *Biophys. J. 83*, 1026 –1038 (2002)

134. Ayton G., A. M. Smondyrev, S.G. Bardenhagen, P. McMurtry, and G.A. Voth. Calculating the bulk modulus for a lipid bilayer with nonequilibrium molecular dynamics simulation. *Biophys. J.* 82, 1226-1238 (2002)

135. Horner D.S., B. Heil, T. Happe, and T.M. Embley. Iron hydrogenases – ancient enzymes in modern eukaryotes. *Trends. Biochem. Sci.* 27, 148-153 (2002)

136. Pomès R., and B. Roux. Molecular mechanisms of H^+ conduction in the single file water chain of the gramicidin channel. *Biophys. J.* 82, 2304-2316 (2002)

137. Schumaker M.F., R. Pomès, and B. Roux. A framework model for single proton conductance through gramicidin. *Biophys. J.* 80, 12-30 (2001)

138. Anderson D., R.B. Shirts, T.A. Cross, and D.D. Busath. Non-contact dipole effects on channel permeation. V. Computed potentials for fluorinated gramicidin. *Biophys. J.* 81: 1255-1264 (2001)

139. Cotten M., C. Tian, D.D. Busath, R.B. Shirts, and T.A. Cross. Modulating dipoles for structure-function correlations in the gramicidin A channels. *Biochem.* 38: 9185-9187 (1999)

140. Weast R.C. Handbook of Chemistry and Physics. *CRC Press*, Boca Raton (1989)

141. Horner D.S., P.G. Foster, and T. M. Embley. Iron hydrogenases and the evolution of eukaryotes. Mol. Biol. Evol. 17, 1695-1709 (2000)

142. Cherny V.V., and T.E. DeCoursey. pH-dependent inhibition of voltage-dependent H^+ currents in rat epithelial cells by Zn^{2+} and other divalent cations. *J. Gen. Phys.* 114, 818-838 (1999)

143. Erdey-Grúz T. Transport phenomena in aqueous solutions. John Willey, New York (1974)

144. Cukierman S., E.P. Quigley, and D. S. Crumrine. Proton Conduction in gramicidin A and in its dioxolane-linked dimer in different lipid bilayers. *Biophys. J.* 73, 2489-2502 (1997)

145. Rotikskaya T. I., E. A. Kotova, and Y. N. Antonenko. Membrane dipole potential modulates proton conductance through gramicidin channel: movement of negative ionic defects inside the channel. *Biophys. J.* 82, 865-873 (2002)

146. Edwards S., B. Corry, S. Kuyucak, and S.H. Chung. Continuum electrostatics fails to describe ion permeation in the gramicidin channel. *Biophys. J.* 83, 1348-1360 (2002)

147. Green M.E. Computer simulations and modeling of ion channels. *Methods in Enzymology.* 293, 694-723 (1998*)*

148. Pantoja R., D. Sigg, R. Blunck, F. Bezanilla, and J.R. Heath. Bilayer reconstitution of voltage-dependent ion channels using a microfabricated silicon chip. *Biophys. J.* 81, 2389-2394 (2001)

149. Lindahl E., and O. Edholm. Mesoscopic undulations and thickness fluctuations in lipid bilayers from molecular dynamics fluctuations. *Biophys. J.* 79, 426-433 (2000)

150. DeCoursey T.E., D. Morgan, and V.V. Cherny. The voltage dependence of NADPH oxidase reveals why phagocytes need proton channels. *Nature* 422: 531-534 (2003)

151. DeCoursey T.E. Voltage-gated proton channels and other proton transfer pathways. *Physiol. Rev.* 83: 475-579 (2003)

Key Words: Proton Transfer, Water Wires, Proteins, Membranes, Review

Send correspondence to: Dr Samuel Cukierman, Department of Physiology, Loyola University Medical School, 2160 South First Avenue, Maywood, IL, 60153, USA. Tel: 708-216-9471, Fax: 708-216-6308, E-mail: scukier@lumc.edu